

Pelagic primary production in the coastal Mediterranean Sea: variability, trends and contribution to basin scale budgets

Paula Maria Salgado-Hernanz^{1,2}, Aurore Regaudie de Gioux³, David Antoine^{4,5}, Gotzon Basterretxea¹

¹Department of Marine Ecology, IMEDEA (UIB-CSIC), Miquel Marquès 21, 07190 Esporles, Spain

5 ²Centro Oceanográfico de Baleares, Instituto Español Oceanografía (COB - IEO), Muelle de Poniente s/n, 07015 Palma de Mallorca, Spain

³ODE/DYNECO/Pelagos, Centre de Bretagne, IFREMER, I. Technopôle Brest-Iroise, Pointe du Diable BP70 29280 Plouzané, France

10 ⁴Remote Sensing and Satellite Research Group, School of Earth and Planetary Sciences, Curtin University, Perth, WA 6845, Australia

⁵Sorbonne Université, CNRS, Laboratoire d'Océanographie de Villefranche, LOV, F-06230 Villefranche-sur-Mer, France

Correspondence to: Paula M. Salgado-Hernanz (pmsalgadohernanz@gmail.com)

Abstract. We estimated pelagic primary production (PP) in the coastal (<200 m depth) Mediterranean Sea from satellite-borne data, its contribution to basin-scale carbon fixation, its variability and long-term trends during the period 2002-2016. Annual coastal PP was estimated at 0.041 Gt C, which approximately represents 12 % of total carbon fixation in the Mediterranean Sea. About 50-51 % of this production occurs in the eastern basin, whereas the western and Adriatic shelves contribute with ~25% each of total coastal production. Strong regional variability is revealed in coastal PP, from high-production areas (>300 g C m⁻²) associated with major river discharges, to less productive provinces (<50 g C m⁻²) located in the southeastern Mediterranean. PP variability in the Mediterranean Sea is dominated by interannual variations but overall trend during the study period shows a notable basin scale decline (17%) is observed since 2012 concurring with a period of increasing sea surface temperatures in the Mediterranean Sea and positive North Atlantic Oscillation and the Mediterranean Oscillation climate indices. Long term trends in PP reveal slight declines in most coastal areas (-0.05 to -0.1 g C m⁻² per decade) except in the Adriatic where PP increases at +0.1 g C m⁻² per decade. Regionalization of coastal waters based on PP seasonal patterns reveals the importance of river effluents in determining PP in coastal waters that can regionally increase in up to five-fold. Our study provides insight on the contribution of coastal waters to basin scale carbon balances in the Mediterranean Sea while highlighting the importance of the different temporal and spatial scales of variability.

1 Introduction

Coastal ocean waters (i.e., < 200 m depth) are an important link between the land and the open ocean. They act as a buffer between terrestrial and human influences and the open ocean (Liu et al., 2000). Despite their relatively reduced extension (~7% of ocean surface area; Gattuso et al., 1998), they behold some of the most productive habitats on the planet. Therefore, they have a disproportionate importance in many basin-scale biogeochemical and ecological processes, including carbon and nitrogen cycling, and in the maintenance of marine diversity (Cebrian, 2002; Coll et al., 2010; Dunne et al., 2007). Besides,

biological production of continental shelves supports over 90 % of global fish catches (Pauly et al., 2002; Pauly and Christensen, 1995).

35 Coastal seawaters support high primary production (PP), contributing to some 10 % of global ocean PP and up to 30 % if estuarine and benthic production is considered (Ducklow et al., 2001; Muller-Karger et al., 2005). These high rates of organic productivity occur in the coastal oceans due to the rapid turnover of the large inputs of nutrients and organic carbon from land. PP drives a significant carbon sink in the ocean (Field et al., 1998; Laws et al., 2000), and is a key regulator of ecological processes such as elemental cycling, trophic structure variabilities and climate change (Bauer et al., 2013; Chavez et al., 2011). In coastal waters, physical and biological processes enhance the carbon transport out of the continental margins into the deep layers of the oceans, thus connecting terrestrial with deep oceanic systems (Cai, 2011; Carlson et al., 2001; Cole et al., 2007). The productivity of coastal sea areas is also of strategic socio-economic importance for many countries considering that PP constrains the amount of fish and invertebrates available to expanding fisheries, a primary resource for many coastal human communities (Chassot et al., 2010). The estimation and understanding of PP evolution and trends in the 40 coastal seas is therefore essential to improve our knowledge of the oceanic carbon cycle.

Scaling up local measurements to estimate the contribution of coastal regions to global carbon fluxes has been hindered by the high spatial and temporal heterogeneity of these waters. Global models of oceanic systems produce carbon fixation estimates with a high degree of uncertainty in coastal regions (Muller-Karger et al., 2005). Coastal waters are complex because of the tight connection between terrestrial and oceanic systems. Terrestrial uploads of nutrients and organic matter 50 originating from groundwater discharges, flash floods or river runoff as well as exchanges with seafloor strongly control the productivity of these waters (Basterretxea et al., 2010; Woodson and Litvin, 2014). The amplitude of seasonal variation of surface chlorophyll (Chl) and surface temperature is often higher on coastal waters compared to the open ocean (Cloern and Jassby, 2008). Furthermore, coastal topography and its interaction with winds, waves and currents generates a high variety of physicochemical niches for phytoplankton growth. Likewise, benthic-pelagic coupling allows the remineralization of nutrients present in shelf sediments during most intense storms. These episodic variations may constitute an important contribution to 55 the overall productivity of shelf waters. Because of the high spatiotemporal heterogeneity in the main coastal subsystems and the concomitant lack of data, most estimated carbon fluxes in these subsystems have relatively high uncertainties (Bauer et al., 2013). In addition, direct human activities and climate change lead to a long-term variation in terrestrial fluxes and coastal biogeochemistry that can potentially have important consequences for the global carbon cycle (Gregg et al., 2003).

60 In the Mediterranean Sea, coastal and shelf areas represent about 21 % of the global basin (259,000 km²), which is a higher contribution than for the global ocean (Pinardi et al., 2006). Although the Mediterranean Sea includes amongst the most oligotrophic areas of the world oceans, it can display marked spatial productivity variations related to the variety of regional climate and oceanographic conditions as well as to the multiple land-derived fluxes that locally fertilize the coastal waters (Goffart et al., 2002). Nutrient-~~inputs-rich~~ rich effluents from human activities in the coast (domestic wastewater, fertilizers, 65 industrial, etc.) and natural river discharges affect continental shelf productivity in this sea, sustaining locally enhanced pelagic and benthic biomass. Nevertheless, the influence of some river flows has been notably reduced by damming affecting water

chemistry and sediment loads and, thereby, the productivity of coastal waters at local and regional scales (Ludwig et al., 2009; Tovar-Sánchez et al., 2016). Moreover, intensive agricultural practices and urbanization have brought unprecedented use and contamination of coastal groundwater (Basterretxea et al., 2010; Tovar-Sánchez et al., 2014). For example, the use of fertilizers
70 has resulted in higher nutrient flowing into the Adriatic and in the lagoons of the Nile river, which has led to eutrophication (Turley, 1999a). However, the impact of this anthropogenic nutrient enrichment may vary between regions, and modelling projections suggest spatial variations in PP as results of climate change.

Accurate quantification of the coastal PP is fundamental for assessment of global carbon cycling in the Mediterranean Sea. Changes in PP have important effects on fish stocks that are socially relevant because of the economical dependency of
75 many Mediterranean coastal communities on marine food products. Several studies have assessed PP at the scale of the entire Mediterranean Sea from satellite remote sensing data (Bosc et al., 2004; Bricaud et al., 2002; Lazzari et al., 2012). However, coastal areas were generally ignored in such studies, so that their contribution to basin scale budgets is still largely unknown. Most coastal studies have a focus on specific regions and/or times (Estrada, 1996; Marty et al., 2002; Moutin and Raimbault, 2002; Rahav et al., 2013). Observed rates of climate change in the Mediterranean basin exceed global trends (Cramer et al.,
80 2018) and future warming in the Mediterranean region is expected to be above global rates by 25 % (Lionello and Scarascia, 2018). Long-term responses of PP in coastal areas to climate forcing remain however uncertain because of the scarcity of adequate field datasets (Gasol et al., 2016).

In this study, we present major characteristics of pelagic PP in Mediterranean coastal waters based on satellite-borne observations for the period 2002–2016. First, we provide global estimations of PP in coastal waters and we assess their
85 contribution to basin scale ~~budgets~~PP, their interannual variability and long-term trends. Then, we regionalize the coastal waters based on their temporal patterns of pelagic PP using Self-Organizing Maps (SOM) and we analyse the contribution of each region to total coastal PP.

2 Materials and Methods

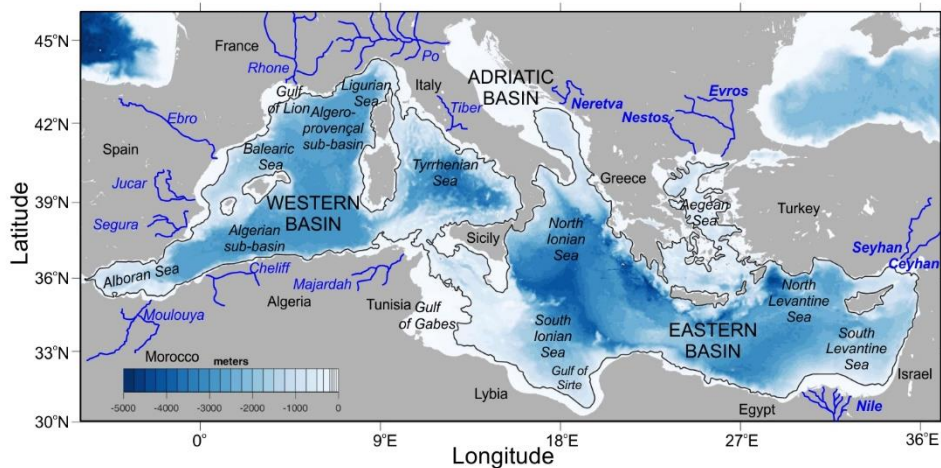
2.1 Remote sensing data

90 We used the Mediterranean Sea Level-3 reprocessed surface chlorophyll concentration product (Chl L3) ~~from multi satellite observations~~, obtained from the EU Copernicus Marine Environment Monitoring Service (CMEMS). This product merges multi-satellite observations, and it is available at 1-day and 1-km resolution (http://marine.copernicus.eu/OCEANCOLOUR_MED_CHL_L3_REP_OBSERVATIONS_009_073). Specifically, the dataset used is 'dataset-oc-med-chl-multi-l3-chl_1km_daily-rep-v02' and the variable name used is
95 'mass concentration of chlorophyll a in sea water (Chl)' obtainable in a NetCDF-4 file format. This Chl L3 dataset is derived by means of the Mediterranean Ocean Colour regional algorithms, that uses with an updated version of the regional algorithm MedOC4 (Mediterranean Ocean-Colour 4 bands MedOC4, Volpe et al., 2019) for pelagic deep Case-1 waters (~~deep~~

pelagic waters, low turbidity) and the AD4 algorithm (ADriatic 4 band; Berthon and Zibordi, 2004; D'Alimonte and Zibordi, 2003) for Case-2 coastal waters (coastal generally shallow and turbid waters, high turbidity waters).

100 Level-2 Sea Surface Temperature (SST, °C) at 1-day and 1-km was obtained from every available orbit from Moderate Resolution Imaging Spectroradiometer (MODIS) aboard satellites-Terra and Aqua satellites. Data were downloaded from the National Aeronautics and Space Administration (NASA) archive website (<http://oceancolor.gsfc.nasa.gov/>), were used for model calculations. Only night-time orbits were selected to avoid problems with skin temperature during daylight. Orbits with quality flags 0 (best), 1 (good) and 2 (questionable) quality flag-2 in SST were included after checking their validity and accuracy in order to have a more complete dataset. Daily (24-hour averaged) Photosynthetically Active Radiation (PAR, in E m⁻²) was obtained as a Level 3 product at 9 km and 1-day resolution. This is the best available resolution at from the NASA archive off from both MODIS and Medium Resolution Imaging Spectrometer (MERIS) data (<https://oceancolor.gsfc.nasa.gov/13/>).

110 _____ All satellite-derived variables were remapped onto a regular 1-km spatial grid over the study area, by averaging all available pixels within each grid cell. For each parameter, outliers were removed whenever they exceeded about 3-times the mean ± SD (standard deviation) of the time series. For the purpose of this study, coastal areas were defined as the waters lying between 5 and 200 m depth. Only values at depths exceeding 5 m depth were considered in order to reduce the possible influence of avoid seafloor vegetation reflectance in any chlorophyll concentration values (Chl, mg m⁻³) at shallow waters bias due to the bottom seagrass reflectance. The analysed time series covers the period from January 2002 to December 2016 for the Mediterranean Sea (30 to 46°N and 6°W to 37°E, Fig. 1).



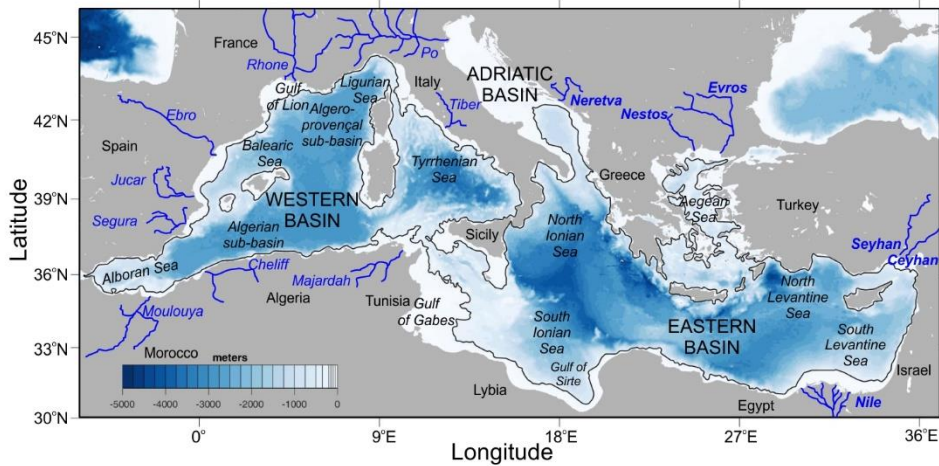


Figure 1: Map of the Mediterranean Sea showing the main basins, sea regions, surrounding countries and major rivers.

120 Bathymetric data were obtained from ETOPO1 (Amante and Eakins, 2009). The black contour indicates the 200m isobath, the limit of coastal waters as defined in the present study.

2.2 Primary production estimates

125 PP was estimated from satellite-derived Chl, SST and PAR values using the time, depth, and wavelength-resolved light-photosynthesis model of Morel (1991).-This model was previously used for estimating PP in the Mediterranean sea (Antoine and André, 1995) and at global scale (Antoine et al., 1996; Antoine and Morel, 1996) and performs well when compared to *in situ* measurements (Campbell et al., 2002; Friedrichs et al., 2009) or when compared to other similar algorithms designed for use with satellite observations (Carr et al., 2006; Saba et al., 2011). Instantaneous production at depth z (m) of the water column, time t of the day, and for absorption of irradiance at wavelength λ , $P(\lambda, z, t)$, is calculated as:

$$130 \quad P(\lambda, z, t) = E(\lambda, z, t) \text{Chl}(z) a^*(\lambda, z) \Phi \quad (\text{mol-gC m}^{-3} \text{s}^{-1}), \quad (1)$$

135 where $E(\lambda)$ is the spectral scalar irradiance for wavelength λ , depth z , and time t of the day ($\text{mol photons m}^{-2} \text{s}^{-1}$), $a^*(\lambda)$ is the spectral chlorophyll-specific absorption coefficient of phytoplankton ($\text{m}^2 \text{mg Chl}^{-1}$), and Φ is the quantum yield of photosynthesis for carbon fixation ($\text{mol C mol photons}^{-1}$; its possible spectral changes are ignored). Note that neither Chl, a^* and Φ are not made variable with time.

The triple integration of (1) w.r.t. wavelength, depth and time gives the daily column-integrated primary production, PP:

$$140 \quad \text{daily PP} = 12 \int_0^D \int_0^{\min(Z_p/Z_b)} \int_{400}^{700} P(\lambda, z, t) d\lambda dz dt (\text{g C m}^{-2}), \quad (2)$$

where the factor 12 is the conversion from moles to grams of carbon, D is the day length or hours of daylight (h), Z_p (m) is the depth where the photosynthetically available radiation (PAR) falls to 0.1% of its value just below the sea surface (so approximately 1.5 times the euphotic depth), and Z_b is the bottom depth taken from the ETOPO1 data base (Amante and
 145 Eakins, 2009). The time integration used intervals equal to 1/30 of the day length (about 20 to 30 min depending on season). The depth integration used intervals equal to 1/50 of Z_p and goes down to whichever is shallower between Z_p and Z_b . The spectral integration is performed over the visible range (400 to 700 nm) with a 5 nm resolution.

The spectral irradiance at a given depth z , $E(\lambda, z, t)$, is calculated as (starting from just below the sea surface):

$$150 \quad E(\lambda, z, t) = E(\lambda, z - dz, t) e^{[-K_d(\lambda, z) dz]}, \quad (3)$$

where the diffuse attenuation for downward irradiance, $K_d(\lambda, z)$ (m^{-1}), is computed as a function of chlorophyll following Morel and Maritorena (2001):

$$155 \quad K_d(\lambda, z) = K_w(\lambda, z) + \chi(\lambda) \text{Chl}(z)^{e(\lambda)} \quad (4)$$

Details about how values are assigned to the parameters a^* and Φ , their dependence on temperature, and other features of this Net Primary Production model (NPP), are to be found in Morel (1991) and Morel et al. (1996).

160 Daily PP calculation was performed every 7 days (starting at day 4), using the averaged Chl for a 7-day window from day-3 to day+3 and for 1 grid point out of 3. Therefore, PP model was run with 8-days resolution and for 1 pixel out of 3 pixels. Later, daily PP data was interpolated to 1-day 1-km grid. Monthly PP data and its anomalies were derived from the above-mentioned dataset.

The model was operated both for clear sky conditions and for the actual MODIS PAR values, in which case a
 165 reduction of the clear-sky irradiance is uniformly applied across the entire day, as being the ratio of the satellite to clear-sky PAR daily values. Chl is assumed to be uniformly distributed with depth, and equal to the satellite-derived value. This simplification was considered more appropriate for the generally shallow and well-mixed waters of coastal areas than the use of global parameterization of the shape of the vertical profile as a function of the surface Chl value (e.g. Morel and Berthon, 1989; Uitz et al., 2006), whose validity outside of open ocean waters is not established.

170 From PP estimates, new (PP_{new}) and regenerated (PP_{reg}) production were calculated using the ratio of export production to total production (i.e., ef -ratio) (Laws et al., 2000; 2011). Indeed, assuming a steady state, the export production

must equal the new production fuelled by new nutrients brought to the surface layers. The *ef*-ratio as a function of satellite-derived temperature and production can be obtained from the empirical relationship obtained by Laws et al. (2011):

175

$$ef = \frac{(0.5857 - 0.0165 T) PP}{(51.7 + PP)} \quad (5)$$

$$PP_{\text{exp}} = PP_{\text{new}} = PP \times ef \quad (6)$$

180 $PP_{\text{reg}} = PP - PP_{\text{new}} \quad (7)$

where T is temperature in degrees Celsius (°C) and PP is the daily production (mg C m⁻²).

185 As shown in Table 1, we report ~~PP annual~~ ~~PP mean~~ neither as vertically integrated values (PP_{annual}, in g C m⁻²), spatially integrated PP estimates for certain basins or regions (ΣPP, in Gt C) or as mean volumetric values (PP_{VOL}, in g C m⁻³). The coefficient of variation (CV) has been estimated for PP as the ratio of the standard deviation to the mean. ~~and surface volumetric PP (PP_{VOL}_{annual}, in g C m⁻³) for the entire Mediterranean coastal areas (PP_{coast}) and also separately for the coastal basins Western, Eastern and Adriatic basins (PP_{basin}).~~ While some authors include the Adriatic in the eastern basin (e.g. Bosc et al., 2004), we treated this region separately because its peculiarities (i.e. bathymetry, influence of rivers, eutrophic character) differentiate it from the rest of the Mediterranean Sea (Cushman-Roisin et al., 2001). Most of the Adriatic has a shallow (<200 m) bathymetry and it collects some 30% of the freshwater flowing into the Mediterranean, acting as a dilution basin for the nutrients discharged by the Po and other Adriatic rivers and becoming one of the most human-impacted regions of the Mediterranean Sea (Ludwig et al., 2009; Micheli et al., 2013; Raicich et al., 2013a)

195 Table 1. Primary production acronyms used in this study, their units and definitions.

<u>Variable</u>	<u>Units</u>	<u>Definition</u>
<u>P</u>	<u>gC m⁻³ s⁻¹</u>	<u>Instantaneous production at each depth (z) of the water column</u>
<u>PP</u>	<u>gC m⁻²</u>	<u>Daily primary production per surface unit. Integration of P over depth and daylength</u>
<u>PP_{annual}</u>	<u>gC m⁻²</u>	<u>Annual mean production per surface unit</u>
<u>ΣPP</u>	<u>GtC</u>	<u>Total carbon fixation per year within a basin or specific region</u>
<u>PP_{VOL}</u>	<u>gC m⁻³</u>	<u>Mean volumetric primary production. Column-integrated PP divided by whichever is shallower of the bottom depth or the productive layer</u>
<u>c</u>	<u>gC m⁻²</u>	<u>New production (i.e., from allochthonous sources)</u>
<u>PP_{reg}</u>	<u>gC m⁻²</u>	<u>Regenerated production</u>

2.3 Coastal regionalization

We used a two-step classification procedure to define coastal regions along the Mediterranean based on their temporal PP patterns. First, 9 regions (R1 to R9) were identified using a classification technique based on an unsupervised learning neural network (Self-Organizing Maps or SOM; Kohonen, 1982; 2001). Then, 18 alongshore marine ecoregions were obtained considering the most relevant cross-shore limits of the SOM-derived regions (Z1 to Z18).

SOM is an unsupervised neural network method that reduces the high dimensional feature space of the input data to a lower dimensional network of units called neurons. SOM is especially suited to extract patterns in large datasets of satellite data (Ben Mustapha et al., 2014; Charantonis et al., 2015; Farikou et al., 2015). Unlike other classification methods, like k -means, SOM tends to preserve data topology (i.e. preserves neighbouring regions) and, therefore, it is particularly suited for pattern recognition (Liu and Weisberg, 2005). It allows adequate classification of areas with high spatial complexity and strong gradients. Similar neurons are mapped close together on the network facilitating the visualization of patterns and a topological ordination of the classified areas and the relative distance among neurons is obtained as results of the analysis.

For typical satellite imagery, SOM can be applied to both space and time domains. Here, we have addressed the analysis in the time domain of the datasets, which allows regionalizing the studied area on the basis of similarities in the time variation of PP. We chose a map size of (3 x 3), with 9 neurons (for further details, see Basterretxea et al. 2018). We used a hexagonal map lattice in order to have equidistant neighbours and to avoid introducing anisotropy artefacts. For the algorithm initialization, we opted for linear mode, batch training algorithm, and 'ep' type neighbourhood function since this parameter configuration produces the lower quantitative and topological error and computational cost (Liu et al., 2006). These SOM computations were performed using the MATLAB toolbox of SOM v.2.0 (Vesanto et al., 2000a, 2000b) provided by the Helsinki University of Technology (<http://www.cis.hut.fi/somtoolbox/>).

2.4 Climate data

To identify possible drivers of long-term PP variability we searched for correlations with two climate indices, the North Atlantic Oscillation index (NAO) and the Mediterranean Oscillation Index (MOI). The corresponding data were downloaded from the Climate Research Unit at the University of East Anglia (<https://crudata.uea.ac.uk/cru/data/>) in monthly resolution. Climate indices are defined either as anomalies of a climate variable, using the difference between two geographical points, or as principal components (Hurrell, 1995).

NAO is the central mode of climate variability of the Northern Hemisphere atmosphere. It is based on the pressure difference between the middle of the North Atlantic Ocean and Iceland, which affects winter conditions in the North Hemisphere (Hurrell and Van Loon, 1997; Marshall et al., 2001). Positive NAO results in a relatively dry winter in the Mediterranean but a warmer and wetter winter in northern Europe, and *vice versa*. Because of its influence on precipitation, Mediterranean river inflows are generally anti-correlated with the NAO (Trigo et al., 2006).

MOI is the most widely used teleconnection index for the Mediterranean basin. It reflects differences in temperature, precipitation, circulation, evaporation and other parameters between the eastern and western basin. There are different versions depending on the points of reference (Criado-Aldeanueva and Soto-Navarro, 2013). We used the version obtained as the normalized pressure difference between Gibraltar and Israel (Palutikof, 2003). Positive MOI phases are associated with increased atmospheric pressure over the Mediterranean Sea that promotes a shift of the wind trajectories toward lower latitudes leading to milder winters (Criado-Aldeanueva and Soto-Navarro, 2013). Under these conditions, reduced precipitation is observed in the southeastern Mediterranean region (Törnros, 2013). With some regional differences, NAO and MOI express relatively similar climate patterns over the Mediterranean Sea. They are highly positively correlated in winter, and weakly but still significantly correlated in summer (Efthymiadis et al., 2011; Martínez-Asensio et al., 2014).

2.5 Statistical analyses

Linear temporal trends in the PP series were calculated using Theil-Sen slope adjustment (Sen, 1968) of the residuals of the de-seasonalized series. Time series have been de-seasonalized by removing the 8-day climatological mean for the original time series. Time series with >12% of missing values were excluded from the analysis and the analysis was calculated pixel by pixel. A Mann-Kendall statistics test is applied to each pixel and only pixels with a trend statistically significant at the 95% level were considered (Salmi et al., 2002). Only pixels with a trend statistically significant at the 95% level were considered. The use of this non-parametrical test is suitable for non-normally distributed data and has been previously used in the trend examination of remote-sensing Chl time series (Colella et al., 2016; Kahru et al., 2011; Salgado-Hernanz et al., 2019).

245 3 Results

3.1 Coastal primary production

Annual primary production in coastal waters of the Mediterranean Sea (ΣPP_{Coast}) is estimated to be 0.041 ± 0.004 Gt C, which represents some 12% of total carbon fixation in the Mediterranean Sea (see Table 4-2 and 23). Approximately, 80% of this ΣPP_{Coast} is sustained by recycling processes and, the rest, PP_{new} , is exported to the seafloor or to nearby areas. Although average surface Chl concentration is 3-fold higher in coastal areas (0.3 mg m^{-3}) than in open areas (0.11 mg m^{-3}), the annual carbon fixation per surface area (PP_{annual}) over the shelf is, on average, 26% lower than in the open ocean (100 ± 91 and $136 \pm 40 \text{ g C m}^{-2}$ respectively; see Table 4-2 and 23). We would have expected that Mediterranean coastal annual PP would also be higher (about 1.7 fold) than oceanic annual PP. This hypothesis would have been observed if the lower PP_{annual} values in the coast are depth integration in coastal areas would have been down to Z_p . However, due to depth integration in coastal areas is being quite often stopped at a much shallower depths, i.e. $Z_b < Z_p$, hence the lower PP per unit area. The surface volumetric PP ($PP_{\text{VOLannual}}$) has been also estimated with a mean value of $2.93 \pm 9.60 \text{ g C m}^{-3}$ (Table 1). Although precise comparisons with offshore values are difficult due to scarcity of published surface PP_{VOL} , $PP_{\text{VOLannual}}$, it can be estimated that this value volumetric production is between 2.5 and 33.2 higher than oceanic values (assuming Z_p 120-150 m). This mean value

of volumetric productivity could not have been compared with oceanic productivity in the Mediterranean Sea considering that previous works presented only integrated production (e.g. Azov, 1986; Bosc et al., 2004; Bricaud et al., 2002a; Coll et al., 2010; Krom et al., 1991; Macias et al., 2015).

Figure 2 reveals ~~some the~~ differences in ~~PP_{annual}~~. ~~PP are observed~~ between the more productive shelf waters in the western basin and those in the eastern basin ($PP_{\text{annual}}=9890\pm55.39$ g C m⁻² and 9273 ± 96.86 g C m⁻², $p<0.001$). The Adriatic shelf ~~being is~~ by far the most productive, ~~particularly if mean values are considered~~ ($PP_{\text{annual}}=1243\pm106.76$ g C m⁻², ~~Table 4~~ ~~Table 2~~). Annual carbon fixation is 97% higher in the eastern ($\Sigma PP_{\text{east}}=0.021\pm0.002$ Gt C) than in the western shelf ($\Sigma PP_{\text{west}}=0.011\pm0.001$ Gt C), which is due to greater eastern surface area (about twice the western surface area; ~~Table 1~~ ~~Table 2~~). ~~PP_{annual} varies spatially from 90 to 250 g C m⁻² in the western shelf, and from 50 to 400 g C m⁻² in the eastern basin where lowest values (<75 g C m⁻²) are found mainly along the Gulf of Sirte.~~ Contrastingly, ~~PP_{annual} exceeds 100 g C m⁻² in the Adriatic basin reaching values above 400 g C m⁻² in the north western Adriatic coast (Fig. 2b).~~ The most productive coastal regions (>150 g C m⁻²) are ~~mainly located along the European coasts in and seem to be related regions enriched by with the outflow regions of major river outflows.~~ Indeed, the highest values of the coefficient of variation of primary production (CV_{PP}) are observed in the mouth of the Nile, Ebro, Rhone, Tiber, Po, Neretva or Nestos/Evros rivers. ~~In addition However Nevertheless, in some coastal regions of the eastern basin, high primary production values are also observed in the like the Gulf of Gabes and the Nile Estuary primary production is also outstandingly high (> 300 g C m⁻²) of the eastern basin where the lowest values (<75 g C m⁻²) are found mainly along the Gulf of Sirte.~~ Along the western ~~n~~North African coast, ~~PP_{annual} also~~ displays values >150 g C m⁻²; however, since the shelf is narrow, its contribution to ΣPP_{Coast} is marginal (Fig. 1 and Fig. 2). The annual volumetric productivity follows a similar pattern than the annual integrated production with most values varying between 1-3 g C m⁻³ but reaching up to > 10 g C m⁻³ in the most productive coastal regions of the Adriatic Sea and the Gulf of Gabes (Fig. 3a). ~~The Coefficient of Variation of PP values, both per surface or per volume unit, were calculated dividing the standard deviation (SD) value by its corresponding mean PP value.~~

Table 12. ~~Surface area and the correspondent basin percentage to chlorophyll mean surface area, (Chl) ± standard deviation (SD), ΣPP , the correspondent basin percentage % to ΣPP_{Coast} (% ΣPP_{Coast}), PP_{annual} median ± SD (PP_{annual} mean), and PP_{VOL} median ± SD (PP_{VOL} mean) Basin extension, chlorophyll and pPrimary production for the Mediterranean Sea, open ocean waters, and coastal waters during the period 2002–2016. For ΣPP and PP_{annual} , Mediterranean Sea values were obtained summing open ocean waters values to coastal waters values. Surface area, annual mean surface mean chlorophyll (Chl), ΣPP for each basin annual average and correspondent % to ΣPP_{Coast} , PP (PP_{annual}), annual integrated PP (ΣPP) and annual average productivity per unit volume PP (PP_{VOL} , PP_{VOL} annual) PP values are shown as median. Values are represented as Mean Average ± Standard Deviation (mean (SD) values are indicated for each mean value.~~

	Surface area (10 ³ km ²) (%)		Chl (mg m ⁻³)	ΣPP (Gt C)	% of ΣPP _{Coast}	PP _{annual} (g C m ⁻²)	PP _{VOL} (g C m ⁻³)
Mediterranean Sea	2,504		0.19±0.78*	0.349±0.118***		140±40**	
Open ocean waters	1,975		0.11±0.18*	0.308±0.118		136±40**	
Coastal waters	529	100	0.30±0.17	0.041±0.004	100	83±75 (100)	1.16±9.60 (2.93)
Western coast	141	27	0.21±0.14	0.011±0.001	25	90±39 (98)	1.23±2.61 (1.59)
Eastern coast	287	54	0.30±0.16	0.021±0.002	51	73±86 (93)	1.01±11.8 (3.34)
Adriatic coast	101	19	0.39±0.23	0.010±0.001	24	99±76 (124)	1.50±7.23 (3.27)

	Surface area (10 ³ km ²) (%)	Chl (mg m ⁻³)	PP _{annual} (g C m ⁻²)	PPVOL _{annual} (g C m ⁻³)
Mediterranean Sea	2,504	0.19±0.78*	140±40**	
Open ocean waters	1,975	0.11±0.18*	136±40**	
Coastal waters	529	0.30±0.17	100±91	2.93±9.60
Western shelf	141	0.21±0.14	98±55	1.59±2.61
Eastern shelf	287	0.30±0.16	92±96	3.34±11.84
Adriatic shelf	101	0.39±0.23	123±106	3.27±7.23

* Mean-Mean surface Chl values obtained by averaging the 8-days and 4-km resolution of surface satellite Chl values obtained from CMEMS (Salgado-Hernanz et al., 2019).

** PP estimated by averaging published satellite data shown in [Table 2](#)[Table 3](#).

*** ΣPP estimated [adding coastal waters data from this study to open ocean waters data taken obtained from Table 2](#)[Table 3](#), [from published data for open ocean waters and values from the present study.](#)

Table 2[Table 3](#). Compilation of published values of **annual PP (PP_{annual})** and **spatially integrated PP (ΣPP)** estimations for the different Mediterranean basins

Region	Period (years)	PP _{annual} (gC m ⁻²)	ΣPP (Gt C)	Method	Reference
<u>Global/Whole Mediterranean estimation</u>	-	80 - 90		<i>In situ</i> (¹⁴ C method)	(Sournia, 1973)
	1981	94±60 - 117.5±75 ^a		Satellite (CZCS)	(Morel and André, 1991)
	1979-1983	125 - 156 ^a	0.308-0.385 ^a	Satellite (CZCS)	(Antoine and André, 1995)
	1997-1998	190		Satellite (SeaWiFS)	(Bricaud et al., 2002)
	1998-2001	79.1 - 88.4		Satellite (SeaWiFS)	(Colella et al., 2003)
	1998-2001	130 - 140		Satellite (SeaWiFS)	(Bosc et al., 2004)
	1998-2007		0.5	Satellite (SeaWiFS)	(Uitz et al., 2010)
	1998-2013	116		Satellite (5 sensors)	(O'Reilly and Sherman, 2016)
Western Basin	1980-1985	120		<i>In situ</i> (Oxygen)	(Bethoux, 1989)
	1981	157,7		Satellite (CZCS)	(Morel and André, 1991)
	1979-1983	157 - 197 ^a		Satellite (CZCS)	(Antoine and André, 1995)
	1996	140 - 150		<i>In situ</i> (¹⁴ C data)	(Conan et al., 1998)
	1997-1998	198		Satellite (SeaWiFS)	(Bricaud et al., 2002)
	1991-1999	83 - 235		<i>In situ</i> (¹⁴ C method)	(Marty et al., 2002)
	1996	175		<i>In situ</i> (¹⁴ C method)	(Moutin and Raimbault, 2002)
	1997-1998	123		<i>In situ</i> (¹⁴ C method)	(Van Wambeke et al., 2004)
	1997-1998	152		<i>In situ</i> (¹⁴ C method)	(Lefèvre et al., PANGEA 2001)
	1998-2001	93.8 - 98.8		Satellite (SeaWiFS)	(Colella et al., 2003)
	1998-2001	163±7		Satellite (SeaWiFS)	(Bosc et al., 2004)
	2006-2007	858 ^{c,d}		<i>In situ</i> (dark-light method)	(Regaudie-De-Gioux et al., 2009)
Eastern Basin (including Adriatic)	1980-1985	137 - 150 ^b		<i>In situ</i> (Phosphorous)	(Béthoux et al., 1998)
	1981	109.4		Satellite (CZCS)	(Morel and André, 1991)
	1979-1983	110 - 137 ^a		Satellite (CZCS)	(Antoine and André, 1995)
	1997-1998	183		Satellite (SeaWiFS)	(Bricaud et al., 2002)
	1996	96		<i>In situ</i> (¹⁴ C data)	(Moutin and Raimbault, 2002)
	1998-2001	69.1 - 81.5		Satellite (SeaWiFS)	(Colella et al., 2003)
	1998-2001	121±5		Satellite (SeaWiFS)	(Bosc et al., 2004)
	2006-2007	521 ^{c,d}		<i>In situ</i> (dark-light method)	(Regaudie-De-Gioux et al., 2009)
Adriatic Basin	1978-1983	241 - 301 ^a	0.0235	Satellite (CZCS)	(Antoine and André, 1995)
	1998-2001	92.4 - 104.4		Satellite (SeaWiFS)	(Colella et al., 2003)

^aThe estimates from Antoine et al. (1995) and Morel and André (1991) have been corrected by a factor of 1.25 as recommended by Morel et al. (1996).

^bFrom Colella et al. (2003), who estimated it using *f*-ratios (the ratio between new and total PP) obtained from Boldrin et al., (2002).

^cDaily PP (mgC m⁻² d⁻¹) converted to annual PP (mgC m⁻² y⁻¹) multiply by 365.

^dConversion to carbon unit using photosynthetic quotient PQ =1.

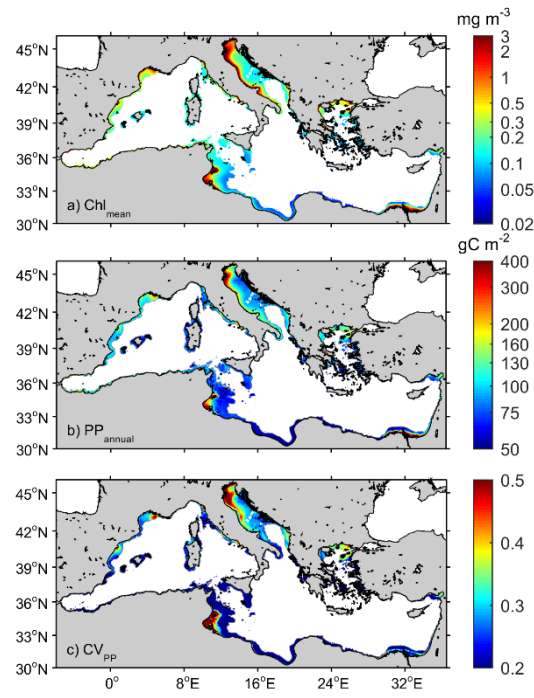


Figure 2: Mean distribution of a) mean-chlorophyll (Chl_{mean} , in mg m^{-3}), b) annual PP ($\text{PP}_{\text{annual}}$)-primary production, in (g C m^{-2}) and, c) coefficient of variation of PP values (CV_{PP}).

315

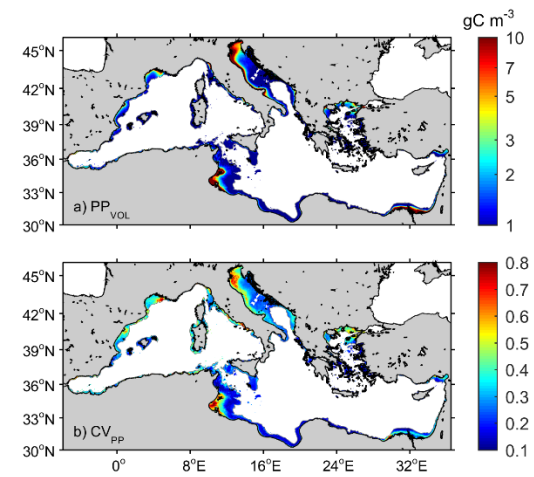


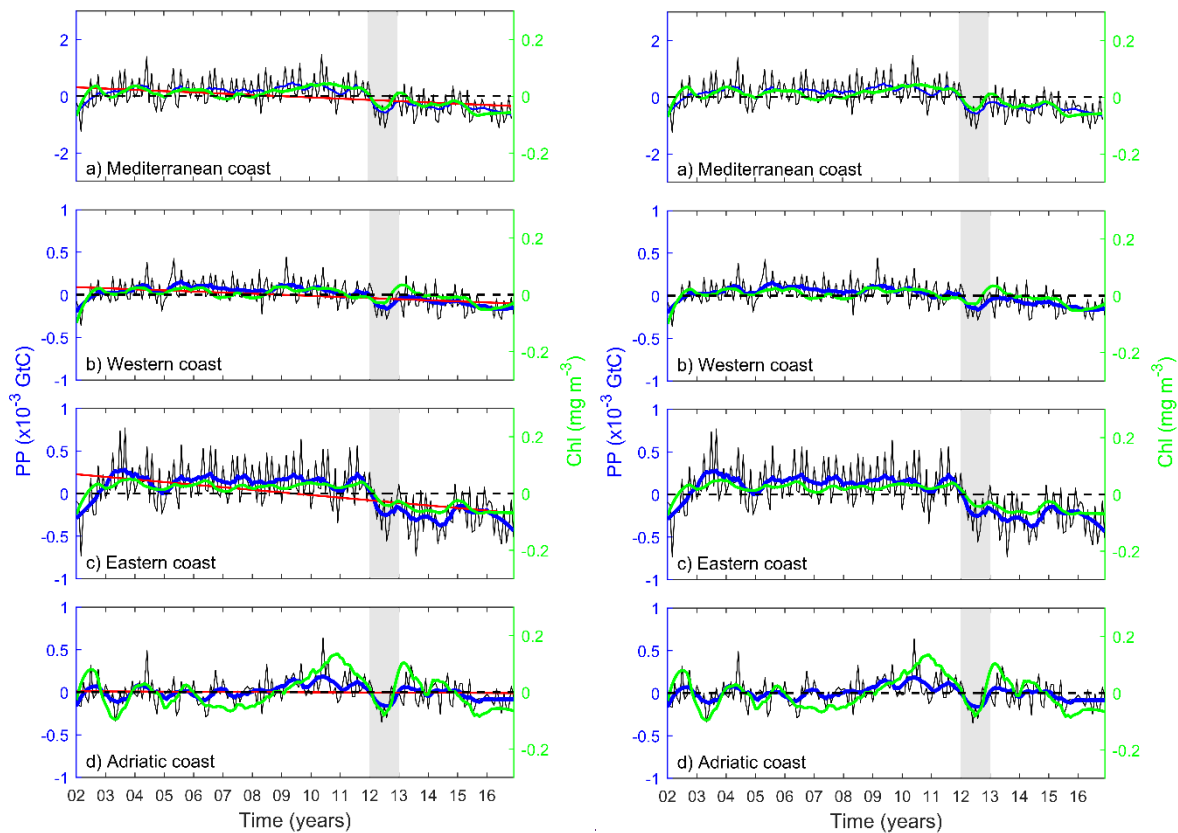
Figure 3: Mean distribution of a) volumetric PP (PP_{VOL} -volumetric primary productivity production in (g C m^{-3}) and b) coefficient of variation of productivity-volumetric PP values (CV_{PP}).

320 3.2 Long-term variability and trends

As shown in Fig. 4, variability in annual PP is dominated by short-scale variations (i.e. subdecadal). The interannual variability is indicated by the low frequency signal of the monthly mean anomalies. The filtered low frequency signal to the anomalies of Σ PP and Chl has been calculated using the Matlab *smooth* function and applying the *sgolay* filter, which uses the Savitzky-Golay method, with a polynomial span *degree* of 17. This degree was therefore filtering about 8 months before and after every

325 time step (about 1.5 years), showing then interannual variability. Σ PP_{Coastal} exhibits moderate interannual variability (up to 25%) whereas basin scale interannual variations range from 26% in the Adriatic basin, up to 28% in the western basin and 29% in the eastern basin. This value of interannual variability was calculated subtracting the year with the minimum annual PP to the year with the maximum annual PP and then dividing this value by the mean annual PP. When considering the whole basin, positive anomalies in Σ PP_{Coastal} ~~eastal~~ PP extended between 2004 and 2011 (mean 0.044 ± 0.001 Gt C y^{-1} ; Fig. 4a).

330 Conversely, year 2012 was particularly unproductive in all three basins (~~specific annual mean PP for 2012 were~~ -0.037 Gt C y^{-1} for the whole basin, 0.010 Gt C y^{-1} for the western, 0.019 Gt C y^{-1} for the eastern and 0.009 Gt C y^{-1} for the Adriatic basin). This negative anomaly marked the beginning of a less productive period, particularly noticeable in the eastern basin (Fig. 4c and Supp. Fig 1 and 2). PPannual ($g\ C\ m^{-2}$) and Σ PP (Gt C) at every year is shown in Supp. Fig 1 and Supp. Fig 2.



335

Figure 4: PP variability and trends for coastal waters in a) the whole Mediterranean Sea, b) western basin, c) eastern basin and d) the Adriatic coast. Black solid lines indicate the original monthly $\Sigma\text{PP}_{\text{Coastal}}$ anomalies and the filtered low frequency signal is overlaid in blue (16-month width *sgolay* filter). Green solid lines indicate the filtered low frequency signal for Chl anomalies (mg m^{-3}). The red line indicates the PP trend during the analysed period (2002–2016) and the grey band indicates year 2012.

340

Long term trends in PP at 95% of confidence level are significant at basin scale and also in the western and in the eastern basins ($p < 0.05$; Fig. 4a-c) whereas the Adriatic Sea does not display significant trends. However, while a slight negative tendency is seen in the western coast (-10.73 TC per decade; Fig. 4b), a more dramatic tendency, driven by a shift in year 2012, is observed in the eastern basin (-25.39 TC per decade; Fig. 4c). As revealed by Fig. 5a, some regionally coherent patches of significant trend in PP are observed along the coast. Most of these regions presented declining PP trends, particularly along the north African coast where SST temperature is increasing at a higher rate (Fig. 5b). Typical PP trend magnitudes observed along the Spanish Mediterranean and the North African coast from the Gulf of Gabes range from -0.05 to $+0.05 \text{ g C m}^{-2}$ per decade. Some positive PP trends, exceeding $+0.1 \text{ g C m}^{-2}$ per decade, can be determined in some coastal regions of the north of the Adriatic Sea.

350

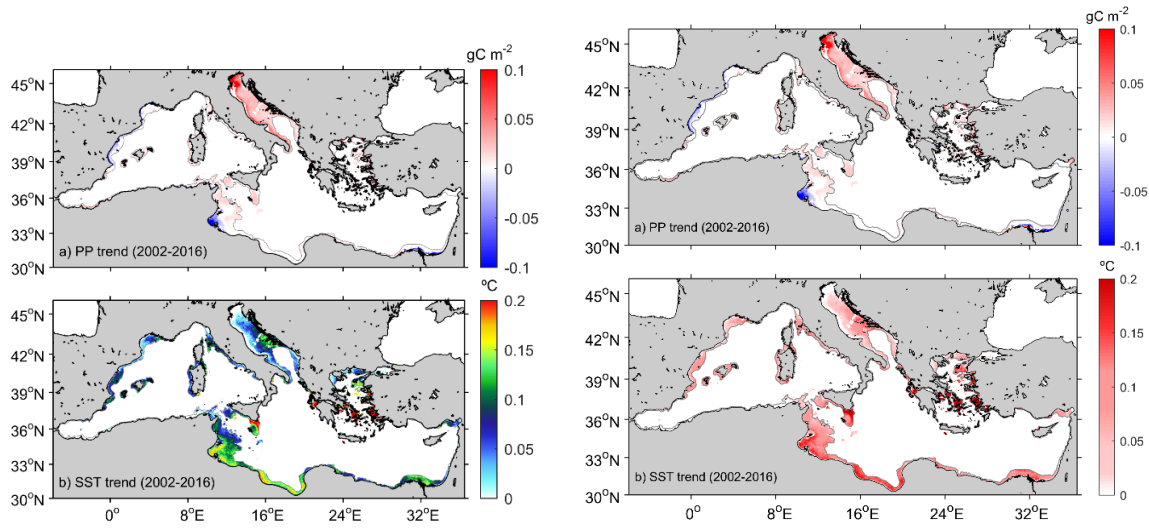


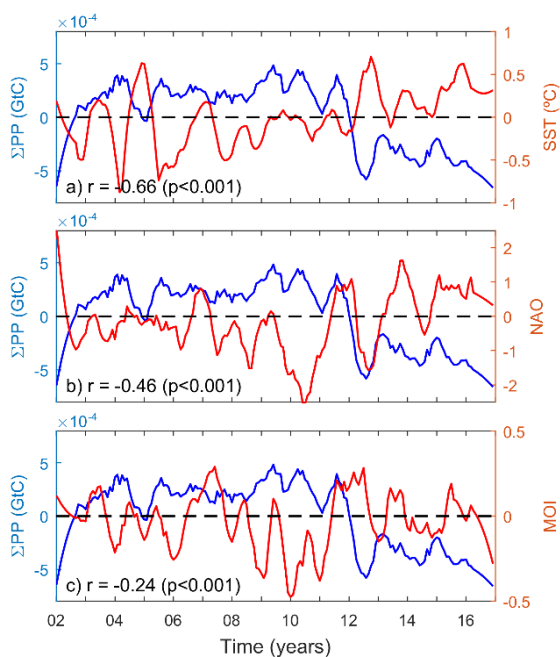
Figure 5: Trends in primary production and sea surface temperature. Values correspond to the change per decade. a) Theil-Sen trend in pelagic primary production estimated from daily values for the 2002–2016 period. b) Trend in SST temperature.

Only significant trends ($p < 0.05$) are shown.

355

A significant negative correlation was observed between coastal monthly anomalies of ΣPP and SST ($r = -0.63$, $p < 0.001$; Fig. 6a) showing that the important decrease of Chl over the years was able to compensate the effect of temperature increase revealing a decrease in phytoplankton biomass as the sea warms up. In addition, we observed evidence of inverse relationship between

360 PP variability and the phase of the climate indices NAO and MOI ($r=-0.45$, $p < 0.001$ and $r=-0.22$, $p < 0.001$ respectively; Fig. 6b-c, [Supplementary Table 1](#)). The response of PP to climate variations varied seasonally. Indeed, NAO influenced coastal PP in summer, both in the western and in the eastern basin ($r=0.25$, $p=0.06$; $r=0.22$, $p=0.08$ respectively) and MOI variations were better correlated with PP global variations in spring ($r=0.28$, $p=0.04$), showing a higher impact in the Adriatic basin ($r=0.37$, $p=0.02$) ([see Supplementary Table 1](#)). No significant correlation was found during the winter nor fall season for any index. Correlation analyses were performed using the Pearson Product Moment correlation. Differences between means were tested using the Kolmogorov-Smirnov test (Massey et al., 1951).

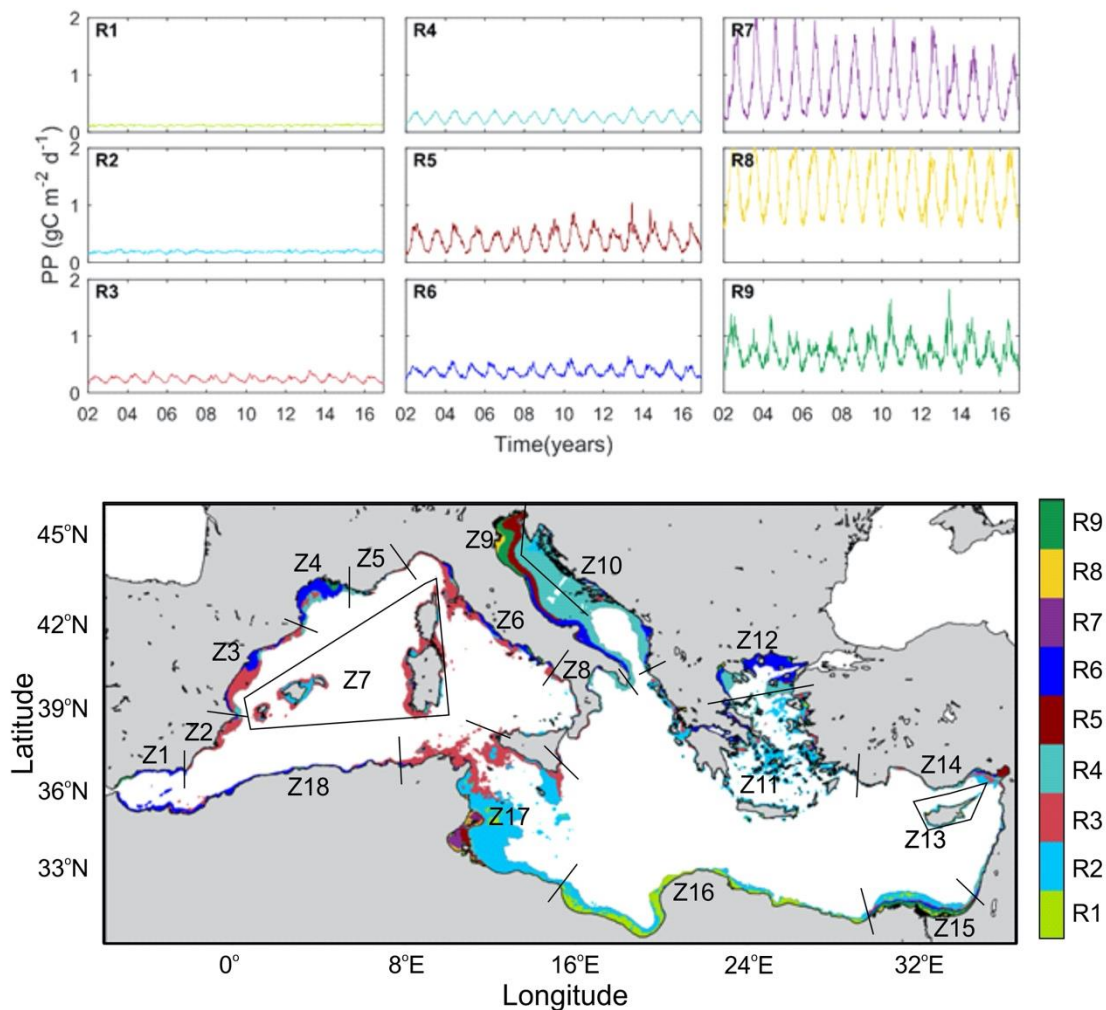


365 Figure 6: Relationship between coastal pelagic primary production (Σ PP [anomalies](#), blue lines) and a) SST anomalies, b) NAO index and c) MOI index (red lines).

3.3 Coastal regionalization

370 The nine characteristic temporal PP patterns, their corresponding spatial distribution obtained from the SOM analysis and the 18 zones in which the coastal region was classified are shown in Fig. 7. Generally, wider shelves present higher spatial complexity manifested as a larger number of SOM patterns. About 78% of the shelf waters include R1, R2, R3 and R4 patterns. In particular, R1 and R2 characterize areas of low production with scarce seasonality ($PP_{\text{annual}}=44\pm 17$ and 69 ± 22 g C m⁻², respectively; Table 3) typically occurring in the southern and eastern Mediterranean (12 and 29% of the total surface area). They are representative of the productivity patterns in vast shelf regions in the Gulf of Gabes and Sirte and in the central 375 Aegean (Z17, Z16, Z14 and Z11). R3 and R4 correspond to higher production and a wider range of variation ($PP_{\text{annual}}=90\pm 32$

and $98 \pm 39 \text{ g C m}^{-2}$; Table 3 and Fig. 7). While R3 (18.6% of total coastal surface) is frequent in shelf regions of the western basin (Z2, Z3, Z5 and Z7), R4 extends over the deepest areas of the Adriatic Sea (Z9 and Z10) Both patterns are representative of variations observed in 36.9% of the coastal waters.



380

Figure 7: Regionalization of the coastal waters in the Mediterranean Sea based on their temporal patterns of pelagic primary production. a) Characteristic temporal patterns of PP obtained from SOM classification (R1 to R9) and b) coastal regions defined from alongshore variations of the SOM – regions (Z1 to Z18).

385

Table 3. ~~Extension and p~~Primary production for each of the SOM-defined regions (R1 and R9). ~~Coastal surface area and its relative contribution to total coastal water surface (%). Mean annual PP (PP_{annual}), annually integrated PP (ΣPP) and its contribution in each SOM defined region to the total coastal PP.~~ Mean annual PP is estimating by averaging mean daily PP and then multiply it by the number of days of the year; i. e., 365.

	Area		PP_{annual}	ΣPP	
	(km ²)	(%)	(g C m ⁻²)	(10 ⁻³ Gt C)	(%)
R1	61,052	12.2	44±17	1.98±0.24	4.8
R2	149,766	29.0	69±22	8.89±0.66	21.5
R3	94,562	18.6	90±32	7.31±0.54	17.6
R4	93,103	18.3	98±39	7.81±0.45	18.8
R5	22,566	5.0	154±102	2.95±0.27	7.1
R6	47,977	9.8	140±70	5.50±0.58	13.3
R7	5,816	1.8	288±217	1.41±0.24	3.4
R8	7,822	2.2	508±283	2.67±0.67	6.5
R9	13,181	3.2	281±175	2.95±0.38	7.1

As shown in Table 3, areas of low production with seasonal patterns R1 to R4 contribute to more than 62% of total pelagic carbon fixation in Mediterranean coastal areas. In contrast, systems of higher production ($PP_{\text{annual}} > 280 \text{ g C m}^{-2} \text{ d}^{-1}$) barely contribute to 17% of total production. These regions of enhanced production are generally constrained to Regions of Freshwater Influence (ROFIs; Simpson, 1997) where terrestrial nutrients fuel coastal production. Indeed, R8 is almost exclusively restricted to the river mouths and it presents elevated PP_{annual} values ($1.29 \pm 0.50 \text{ gC m}^{-2} \text{ d}^{-1}$) and a wide range of variation of 0.67 to 2.14 $\text{gC m}^{-2} \text{ d}^{-1}$. An exception is R7 pattern, which is exclusively located in the shallowest inner shelf of the Gulf of Gabes, and it is bounded by R5, a transition region between the inner and outer shelf. Unlike the other regions, where PP peaks in late winter-spring, maximum PP in R7 occurs in fall. Finally, R5 and R6 patterns correspond to transition regions accounting for 20.4% of the total production and 14.8% of the Mediterranean coast. While R5 mainly occurs in deltas areas, R6 is characteristic of the western Mediterranean shelf, including the North African coast ($0.36\text{-}0.08 \text{ gC m}^{-2} \text{ d}^{-1}$; Fig. 7).

The SOM-based regionalization reveals two groups of coastal waters: those with low cross-shore variability and including only one or two SOM regions (i.e. Z1, Z13, Z16 and Z18) and those with strong cross-shore gradients including several SOM-regions (i.e. Z4, Z9, Z12, Z15). The first pattern is typically observed in narrow continental shelf areas with low influence of river inputs whereas the second group is found in regions with wider continental shelf such as ROFIs (the Rhone delta, the north and western coastline of the Adriatic Sea and the Nile Delta) and in the Gulf of Gabes. The western Adriatic (Z9) and the Gulf of Gabes (Z17) are the largest contributors to ΣPP_{Coast} , contributing together to 35.9% of shelf production in the Mediterranean Sea but, in the case of Z17, it is mainly due to its large extension (Table 4). PP is also high in the northern Alboran Sea (Z1), Nile delta (Z15), the western Adriatic (Z9), and Gulf of Lions (Z4; Table 4). With the exception of Z1, influenced by the entrance of waters from the Atlantic Ocean and by local coastal upwelling, these zones receive important riverine fluxes (Q).

Table 4. Surface, river discharge flow (Q), annual mean PP (PP_{annual}), annual integrated PP (ΣPP) and its contribution respect to the total coastal Mediterranean Sea PP for each of the 18 alongshore zones characterized in the Mediterranean Sea. Mean and standard deviation (S.D.) are calculated from 14 year averages is calculated from 15-year averages (2002-2016).

	Area		Q	$PP_{\text{annual}} \pm S.D.$	$\Sigma PP \pm S.D.$	
	(km ²)	(%)	(km ³ y ⁻¹)	(g C m ⁻²)	(10 ⁻³ Gt C)	(%)
Z1	1,869	0.4	0.5	215 ±124	0.22±0.05	0.4
Z2	7,226	1.4	1.2	107±58	0.62±0.08	1.4
Z3	18,870	3.6	21.4	104±47	1.71±0.16	3.6
Z4	15,196	2.9	57.7	128±72	1.61±0.12	2.9
Z5	878	0.2	1.9	84±33	0.04±0.02	0.2
Z6	20,392	3.9	14.6	101±64	1.62±0.20	3.9
Z7	29,666	5.7	0.5	74±26	1.66±0.20	5.7
Z8	8,178	1.6	3.7	81±34	0.40±0.09	1.6
Z9	64,780	12.4	70.5	140±124	7.63±0.66	12.4
Z10	40,997	7.8	35.8	89±37	2.81±0.25	7.8
Z11	58,252	11.1	21.5	81±59	2.95±0.67	11.1
Z12	25,720	4.9	21.2	123±76	2.25±0.33	4.9
Z13	30,71	0.6	0	53±18	0.09±0.02	0.6
Z14	16,814	3.2	21.3	97±61	1.21±0.14	3.2
Z15	28,544	5.5	17	170±182	4.02±0.50	5.5
Z16	46,065	8.8	0	48±17	1.85±0.12	8.8
Z17	123,071	23.5	1.1	90±87	9.72±0.80	23.5
Z18	13,411	2.6	6.1	125±56	1.24±0.18	2.6

4 Discussion

4.1 Coastal primary production

~~To our knowledge, this is the first~~In this -study we focused on the contribution of coastal waters to the overall pelagic PP in the Mediterranean Sea. While the mean coastal values for the Mediterranean (100±91 g C m⁻²) are somewhat lower than the mean values over the continental shelves of the ~~World~~world ocean (160±40 g C m⁻²; Smith and Hollibaugh, 1993), the impact of coastal pelagic PP to total basin production (12%) is in the high range of the estimations for other Seas (Muller-Karger et al., 2005). This estimation is subject to the uncertainties inherent to using satellite ocean colour, which is limited to the upper ocean (down to 20 m at best in clear waters) and has poor performance in some areas (i.e. Case-2 waters). It nevertheless provides an assessment of net rates of carbon fixation in coastal areas that is consistent with global estimations of the contribution of coastal areas to oceanic production (Gattuso et al., 1998; Ducklow and McCallister, 2004; Muller-Karger et al., 2005). Bias in coastal Chl estimations is mainly due to the presence of non-phytoplankton components such as coloured dissolved organic matter (CDOM) or other terrestrial substances (Morel et al., 2006). These compounds originate from coastal

erosion, resuspension in shallow areas, river inputs or anthropogenic effluents. Likewise, they affect the propagation of photosynthetic radiation through the water column (Morel, 1991). However, the possible uncertainties and biases caused by Chl estimation through satellite data might have alter very weakly our estimation of coastal PP. Indeed, previous studies agreed that ~~Indeed,~~ Case-1 waters are largely predominant in the coastal Mediterranean regions whereas Case-2 waters are reduced to less than 5% of the whole basin (Antoine and André, 1995; Bosc et al., 2004; Bricaud et al., 2002). This constitutes some 23% of the coastal waters with prevalence in the north Adriatic Sea, Gulf of Gabes and around Nile delta. In particular, they are confined to the north Adriatic Sea, Gulf of Gabes and around Nile delta where our PP estimations may present larger uncertainties (Antoine and André, 1995). However, PP_{annual} values off the Nile river delta, >100 g C m⁻² estimated here, are only slightly higher than those reported by Antoine et al. (1995) (80-100 g C m⁻²). Highest values have been reported for this region (>300 g C m⁻²) but, as shown in Fig. 2, they are restricted to a narrow coastal band. In the case of the Adriatic Sea, Umani (1996) reported values of PP from 50 to 200 g C m⁻² y⁻¹, while Zoppini et al. (1995) estimated PP rates from 210 to 260 g C m⁻² y⁻¹ in the northern coastal areas. Our estimations range between 100 and >350 (with mean values of 123±106 g C m⁻²).

Contrary to what we would have expected, we observed that the eastern basin contributes more than the western basin to overall coastal production (51% and 25% respectively; Table 2). Its great extension (twice higher than the western basin) and despite being generally less productive (median PP_{annual} = 73±86 g C m⁻²), because of its extension, and due to the increased productivity in regions like Gabes, the Nile and the northern Aegean Sea may explain greater coastal PP in the eastern basin than in the western basin. Additionally, due to the lack of large shallow and productive areas in the western basin, we observed few volumetric PP values above 30 g C m⁻³ in the western Mediterranean whereas high PP is more frequent in the Adriatic Sea and in the eastern Mediterranean in shallow waters of the Gulf of Gabes and in the Nile Delta. the eastern basin contributes more than the western basin to overall coastal production (50.51% and 25% respectively; Table 1 Table 2). Furthermore, carbon fixation from the Adriatic Sea represents 24% of total coastal production, which is significant considering the area of this Sea (19% of Mediterranean coastal waters). The relevance of the contribution of the Adriatic Sea in overall coastal PP relies in two main characteristics; (1) coastal waters (<200 m) constitute a large part of the Adriatic Sea and (2) about one third of the river discharge in the Mediterranean is concentrated in the Adriatic Sea (see Table 4). Indeed, patterns in the northern Adriatic Sea reflect a variation in the drivers of PP with respect to other regions. For example, while internal processes (i.e. vertical diffusion and mixing), the influence of direct wastewater discharges — and, ~~less so,~~ atmospheric deposition, drive PP in most coastal waters, production in the north Adriatic would be mainly driven by fluvial sources of carbon and regeneration through bacterial pathways (Powley et al., 2016; Rodellas et al., 2015; Umani et al., 2007). Moreover, distinctive dynamics in this sea is driven by the influence of river outflows on stratification and general circulation patterns (Djakovac et al., 2012; Giani et al., 2012).

Regionally, the Alboran Sea, the Gulf of Lion, the Adriatic Sea, and the Aegean Sea the Nile delta and particularly the Gulf of Gabes (up to 23% of total coastal production) are the most productive zones. While some of these productive (i.e. PP_{vol} > 3 g C m⁻³) coastal regions are located in areas affected by river outflows, this type production rapidly decreases in offshore

465 direction (see Fig. 3). Exceptions are the Rhone and the Po, and less so, the Nile which, which influence extends far along the
shelf. Other processes like mesoscale circulation are also important in some of these regions –i.e. Gulf of Lions-, as
470 demonstrated by (Macias et al., 2017). Additionally, the exchanges with the more productive Atlantic and Black Sea waters in
Alboran and in the northern Aegean, and local enrichment processes in the Gulf of Gabes are major contributors to coastal
productivity. Indeed, the Gulf of Gabes constitutes an anomaly in the eastern Mediterranean Basin. Its shallowness (< 50 m
<at 110 km off the coast), unique tidal range (maximum >2 m) promoting vertical mixing and the lack of summer nutrient
exhaustion undoubtedly contribute to its high productivity (Béjaoui et al., 2019).

Notwithstanding the importance of land inputs in the production of coastal Mediterranean waters, From *ef*-ratios, we
estimated that on average only 22 ± 20 % of the production in the coastal Mediterranean Sea is new and the rest is sustained via
regenerated sources (Fig. 8a-c). This PP_{new} value (Fig. 8b) is comparable to the mean organic carbon that sinks to the sea floor
475 (28%) estimated from Muller-Karger et al. (2005) and Pace et al. (1987) but higher than PP_{new} estimations provided by Vidussi
et al. (2001) for oceanic waters in the eastern basin (15% of total production). Contrarily to Vidussi et al. (2001) who estimated
 PP_{new} in the eastern basin, the coastal PP_{new} average here includes both eastern and western basins of the Mediterranean, but
also the highly productive areas in the northern Adriatic. This could explain that the PP_{new} observed here is higher than the one
observed for oceanic waters in the eastern basins. Additionally, high *ef*-ratios (> 0.3) are observed in our case in the areas
480 where nutrient inputs from the Atlantic and river effluents significantly enhance PP_{new} (Fig. 8a). Furthermore, *ef*-ratios present
significant seasonality, varying between 0.26 ± 0.04 in the most productive winter-spring season and 0.15 ± 0.02 in summer,
when the water column is strongly stratified and food web shifts to a more recycling dominated system.

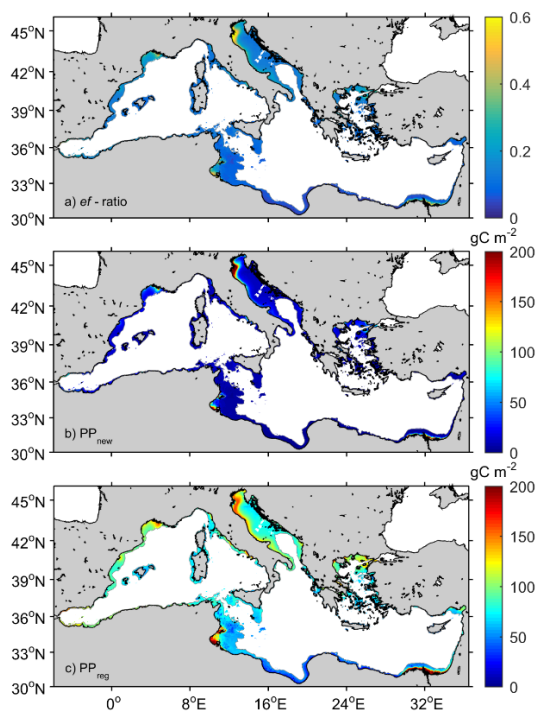


Figure 8. a) *ef*-ratio in coastal waters (<200 m) of the Mediterranean Sea and estimated values of b) new (PP_{new}) and c) regenerated production (PP_{reg}). Mean values for the period 2002-2016.

4.2 Long-term variability and trends

Available satellite ocean colour data span about 20 years, so that temporal trends derived from their analysis are highly depending on decadal variability (Henson et al., 2010). Despite these limitations, satellite observations of ocean colour over the past two decades suggest relationship between warming and reduced productivity in permanently stratified areas (Behrenfeld et al., 2006). Since clear tendencies of warming are observed in the Mediterranean Sea (Nykjaer, 2009; Pastor et al., 2018), intensification of stratification would decrease nutrient supply to phytoplankton and, thus, decrease PP (Behrenfeld et al., 2006; Stambler, 2014).

Barale et al. (2008), using Chl anomalies derived from SeaWiFS remote sensing imaginary data, observed a general decrease in Chl biomass in the Mediterranean Sea over the period 1998–2003. However, some coastal areas in their study displayed the opposite tendency. Macias et al. (2015) anticipated no future global changes of integrated PP in the Mediterranean Sea from modelling results. They predicted a tendency to oligotrophication in the western basin and increase in the productivity of the eastern basin. Our study reveals that $\Sigma PP_{\text{Coastal}}$ in the Mediterranean Sea varies nonlinearly and a reduction of carbon fixation rates is observed since 2012 (Fig. 4a). Overall negative trends are reported here in both the Western and in the Eastern basin (-10.70 and -25.39 TC per decade; Fig. 4b-c). A spatial analysis of the long-term decadal variability reveals weak but spatially coherent and significant tendencies ($p < 0.05$; Fig. 5). In particular, PP declines along the coasts of Spain and Africa. Conversely, trends in some areas of the Adriatic Sea are markedly positive ($> 0.1 \text{ gC m}^{-2}$ per decade) mainly in the proximity of the Po river. While negative tendencies seem to fit with the assumed model of PP limitation associated with increasing temperatures, the origin of the positive trend in the Adriatic basin is more uncertain. A plausible explanation is the variation in the flux ~~or~~ and loads of the northern Adriatic rivers. For example, Giani et al. (2012) observed an increase of the Po River flow with increasing phosphate and dissolved nitrogen concentrations in the Po's delta and its surrounding shelf waters, ~~that could enhance the coastal PP of this region~~. Alternatively, changes the Bimodal Oscillating System (BiOS), i.e. the feedback mechanism between the Adriatic and Ionian (Civitarese et al., 2010) ~~(Civitarese et al., 2010) occurring peaking~~ between 2004 and 2006 ~~in the deep structure of the Mediterranean Sea~~ could have affected mass and nutrient exchanges between the Adriatic and the north Ionian Sea (Font et al., 2007; Schroeder et al., 2008; Šolić et al., 2008; Viličić et al., 2012). In addition, Chl exhibits a strong reduction starting from 2012 that could be the responsible for such trend (Fig. 4-d).

Long-term decadal variations in the eastern and western basins are mostly coupled, suggesting that they share the same PP drivers at this basin scale (Fig. 4b-c). A major feature in the interannual pattern is a global decrease in production in 2012 that is extended to the following years in the eastern basin. Durrieu de Madron et al. (2013) reported peculiar atmospheric conditions in the Mediterranean Sea during 2012 that triggered a massive formation of dense water on the continental shelf and in the deep basin of the Gulf of Lions. A similar anomaly was described in the Adriatic shelf where unprecedented dense water generation was preconditioned by a dry and warm year resulting in a significant reduction of coastal freshwaters and

basin-wide salinity increase (Mihanović et al., 2013; Raicich et al., 2013b). Additionally, Pastor et al. (2018) observed an anomalously temperature increase in the Mediterranean Sea during summer 2012. From our analysis, we infer that this climate-related event had strong influence on the global coastal PP of the Mediterranean Sea.

520 Several studies have reported influence of climate variations in the coast (Belgrano et al., 2008; Cloern et al., 2007; Tiselius et al., 2016). In agreement, we observed an influence of climate scale variability on coastal productivity as suggested by the inverse correlations between Σ PP and SST and, more loosely, with NAO and MOI (Fig. 6). While these correlations emphasize the pre-eminent role of climate variability in the regulation of interannual to decadal scale coastal productivity, the pathways through which this control of the atmosphere over coastal productivity is exerted are complex and may regionally differ (Grbec et al., 2009). Climate can influence phytoplankton growth by the direct effect of temperature on algal metabolism, 525 by changes in basin scale circulation (including exchanges with adjacent seas), by regulating nutrient supply through variations in the thermocline intensity, by changes in wind patterns affecting mixing and dust deposition pathways or through changes in precipitation that have direct influence on wet deposition and on river runoff. These effects are modulated by changes in the biota and in the interaction between organisms (e.g. Molinero et al., 2005). The relative importance of climate-driven processes relative to other productivity enhancing processes depends on regional characteristics and may be seasonally varying. For 530 example, variations in dust deposition, which may sustain up to 50% of new production in the Levantine basin (Kress and Herut, 2001; Herut et al., 2002), are expected to be more important in the eastern and southern Mediterranean coasts because of their proximity to the Saharan dust sources. Likewise, variations in cooling and vertical mixing are expected to be more effective during late winter when PP peaks and when diatoms dominate in the Mediterranean Sea (Lacroix and Nival, 1998; Marty, 2002; Marty and Chiavérini, 2010). 535

Our results reveal that, in contrast to other regions like the North Sea (Capuzzo et al., 2018) or the Arctic Ocean (Gregg et al., 2003), the coastal Mediterranean Sea did not globally display a marked decline in PP during the last decades. We suggest that in some coastal areas, a decrease in vertical nutrient supply though the thermocline may be compensated by other nutrient sources. Variations in atmospheric deposition, groundwater and river outflows together with the influence of human activities through changes in landscape use and [domestic wastewater nutrient](#) management are important sources of 540 nutrient in the ecosystem and thus, act as major drivers of PP in these waters (e.g. Paerl et al., 1999; Powley et al., 2016). As a consequence of human activities, both terrestrial and coastal ecosystems have experienced progressive nutrient enrichment (Conley et al., 2009; Deegan et al., 2012). However, while this effect is evidenced in shallow nearshore waters, its influence in the ocean is estimated to be minimal (Wang et al., 2018). In the Mediterranean Sea, high coast population growth rates and concomitant food demand have resulted in dramatic increase of water demand for irrigation farming and fertilizer use (Ryan, 2008). Indeed, while the freshwater discharge of Mediterranean rivers has significantly reduced during recent decades (~20%), 545 the corresponding total nitrogen inputs to coastal seas are estimated to have increased by a factor up to 5, fuelling PP in river influenced areas (Ludwig et al., 2009). While the importance of groundwater in the Mediterranean Sea could be comparable to that of rivers (Rodellas et al., 2015) and generalized nitrification of Mediterranean coastal aquifers is acknowledged (EEA, 550 1995; Zalidis et al., 2002), general trends in groundwater discharges remain largely unknown.

4.3 Coastal regionalization

Coastal regionalization reveals marked differences in coastal waters PP in the Mediterranean Sea. Annual values range from $215 \pm 124 \text{ g C m}^{-2}$ in the north Alboran Sea (Z1) to $48 \pm 17 \text{ g C m}^{-2}$ along the coasts of Egypt and Libya (Z16). These values are globally lower than published data; yet, literature values in coastal waters are highly variable depending on methodology, depth and/or sampling date. For example, García-Gorrioz and Carr (2001) estimated annual PP of 300-900 g C m^{-2} for Z1 but Morán and Estrada (2001) narrowed this range to mean values between 121 and 366 g C m^{-2} depending on distance from the coast. Pugnetti et al. (2008) reported mean values of 150 g C m^{-2} that are almost twice higher than our values at Z8. In the lower range, Sournia (1973) estimated 30–60 g C m^{-2} in Z16, which is in accordance with our values for this zone. In this sense, despite the limitations inherent to satellite data, the present work provides estimations based on a long data record (14 years) and a homogeneous methodology.

The nine characteristic temporal patterns obtained from the SOM analysis (Fig. 7) reveal small differences in PP among the different regions. Most variations are due to changes in the magnitude of annual carbon fixation, although seasonality little varies. Exceptions are R7, R8 and R9 which represent the dynamics in coastal regions regulated by terrestrial inputs. Likewise, interannual variations are highly coherent among regions, following the basin-scale pattern shown in Fig. 4, including the remarkable decline in productivity during 2012. Exceptions are R1, representing the dynamics in the Gulf of Sirte and R7 in Gulf of Gabes where a different interannual variability suggests alternative sources of PP variability in this region. Indeed, the Gulf of Gabes is a peculiar region displaying consistently high Chl and PP in most studies (e.g. Bosc et al., 2004; Barale et al., 2008). Drira et al. (2008) reported high biomass and toxic dinoflagellate blooms in the inner shelf of the Gulf of Gabes where surface nitrate concentration often exceeded $1 \mu\text{M}$. This enrichment is associated with degradation of the water quality attributed to industrial and urban activities (Hamza-Chaffai et al., 1997; Zairi and Rouis, 1999). However, even though these waters may suffer from eutrophication, satellite-borne data overestimates Chl within these waters, as revealed by Katlane et al. (2011) who observed constant high turbidity and suspended matter of industrial origin affecting these waters but also, reflection from the bottom affecting MODIS data. This suggests that general Chl algorithms may be particularly inaccurate in this region.

The magnitude of coastal PP has been often related to both shelf width and magnitude of river discharge (Liu et al., 2010). Our data does not display a general relationship between shelf width (Q) and $\text{PP}_{\text{annual}}$ (Table 4 and Fig. 9). Indeed, wide shelves with important river discharge flux from the Po, the Rhone and the Nile rivers display high productivity (Z4, Z9 and Z15 $> 170 \text{ g C m}^{-2}$) whereas production is low in narrowest shelves like Z2, Z5 and Z16. However, $\text{PP}_{\text{annual}}$ in some regions with important river inflows, like Z10, are significantly lower ($89 \pm 37 \text{ g C m}^{-2}$). In other regions like Z1 and Z8 PP is high despite the lack of important freshwater sources.

The role of river discharges depends both on Q and on nutrient loads. Most Mediterranean rivers have lost their natural flows and their discharges to the sea are strongly regulated by dams and water abstractions. Consequently, their outflow to the Mediterranean Sea is highly uncoupled from weather and climate variability. For instance, some rivers flowing into the Adriatic

and Ionian Seas, like the Acheloos, Nestos or Aliakmon nowadays present high to maximum discharge in July due to peak
 585 hydropower production (Skoulikidis et al., 2009).

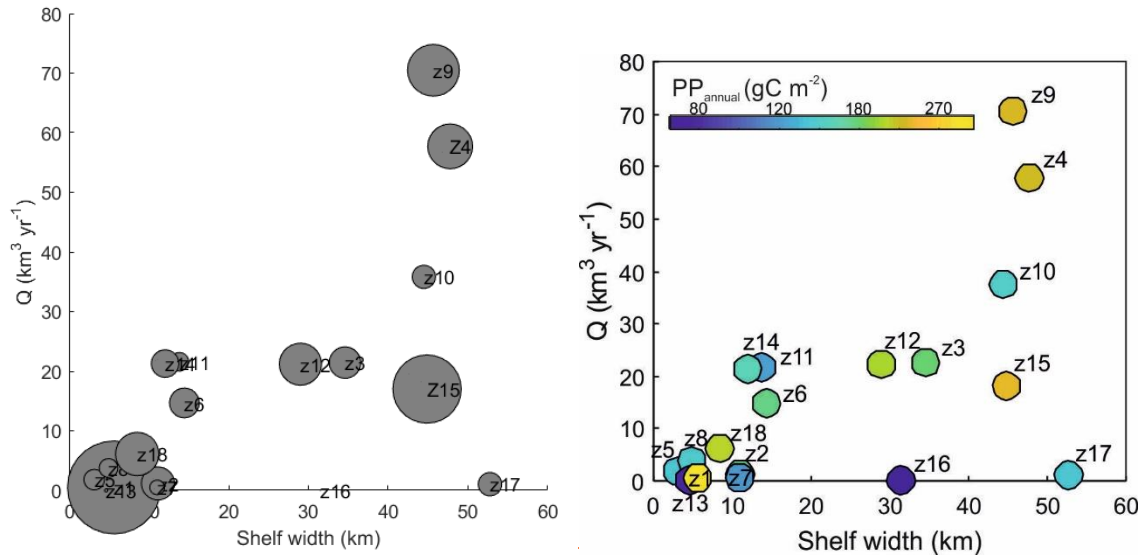


Figure 9: Relation between primary production, shelf width and river discharge flow (Q). Bubbles colours indicates sizes are proportional to the annual mean PP (PP_{annual} (gC m^{-2})) of each of the 18 defined zones (see Fig. 8 and Table 4).

590 Nutrient and organic matter loads have globally increased during the last century (Beusen et al., 2016). Concentrations exported to nearby seas depend on the combined effects of lithology, urban effluents, industry and agriculture in catchment basins that are often difficult to quantify. The Land Use and Land Cover (LULC) data collection provide indices of the threat of potential development for setting land and water quality policies. Rivers like the Rhone and Po with important influence on coastal productivity flow through extensive areas and therefore accumulate the impact from anthropogenic activities.

595 Agricultural practices and urban effluents can strongly determine the concentration and molar ratios of the nutrients flowing into coastal waters. For example, despite the flux of the Nile river has been drastically reduced after the operation of the Aswan Dam (from 47 to 17 $\text{km}^3 \text{y}^{-1}$, Ludwig et al. (2009)), the coastal region is still highly productive. A remarkable increase in the concentrations of nitrate derived from fertilizers and sewage is responsible for this sustained productivity (Turley, 1999; Nixon, 2003, 2004). Conversely, pollution pressures in the western Balkan basins are relatively low and the Neretva (Z10), running

600 through a karstic region in Croatia, displays low nutrient levels (Ludwig et al., 2009; Skoulikidis et al., 2009). Finally, other oceanographic processes determine the productivity of coastal regions. In particular, Z1 and Z18, in the Alboran Sea are comparatively more productive than other areas. The influence of winds and circulation patterns favouring subsurface water upwelling higher productivity in the northern Alboran Sea where described by García-Gorriç and Carr (2001). Also,

605 localized patterns of relatively high primary production were found in persistent deep water density fronts resulting from the interaction of [Modified Atlantic Water \(MAW\)](#) and Mediterranean water by Lohrenz et al. (1988).

5 Conclusions

In summary, pelagic PP in coastal shelves of the Mediterranean Sea during the period 2002-2016 was estimated in this study for the first time using available satellite ocean colour product. We estimated that 12% of PP of the Mediterranean Sea is attributable to coastal pelagic production and from that, about 80% of this carbon fixation is sustained by regenerated pathways.

610 High PP spatial variations were observed among the different regions, as mainly driven by major river effluents, [exchanges with nearby seas \(i.e. Black Sea and the Atlantic Ocean\)](#) and by local processes. Our study shows that some coastal areas are indeed highly productive ($>400 \text{ g C m}^{-2}$) and sustain a large percentage of overall coastal production. Indeed, their temporal variability could be of paramount importance to understand variations in higher trophic levels (e.g. Piroddi et al., 2017). Despite that temporal variability is dominated by interannual and sub-decadal variations, our analysis reveals a weak global negative

615 PP trend in the Mediterranean Sea related to climate driven patterns (i.e., temperature increase). Our analysis also reveals a weak negative PP trend, which cannot be qualified as climate-driven because most of the temporal variability is dominated by interannual or sub-decadal variations and the satellite record is only 14-year long. Nevertheless, long-term effects can be regionally variable (i.e. PP trends in the Adriatic Sea are positive) and variations in ~~of decreases~~ fluvial nutrient inputs, together with other processes such as ocean warming in coastal regions, including heat waves, deserve a closer look as longer ocean

620 colour databases becomes available. Finally, we identify 18 along-shelf zones based on their temporal PP patterns. Two main PP groups were observed: zones with strong cross-shore gradients, typically found in wider estuarine regions and homogeneous zones within narrow continental shelf areas. [These two types of coastal waters clearly characterize the coastal area of a sea where coastal waters are otherwise strongly influenced by ocean conditions.](#)

Competing interests

625 The authors declare that they have no conflict of interest.

Author contribution

GB and AR designed the study in collaboration with DA. PMS and DA conducted most of the analyses. PMS wrote the manuscript, with contributions from all co-authors.

Acknowledgments

630 We are grateful to National Aeronautics and Space Administration, NASA (<https://oceancolour.gsfc.nasa.gov/>) and EU Copernicus Marine Environment Monitoring Service, CMEMS (<http://marine.copernicus.eu/>) for the freely available ocean-color remotely-sensed data. Climate indices were obtained from the Climate Research Unit at the University of East Anglia (<https://crudata.uea.ac.uk/cru/data/>).

Financial support.

635 This article is a result of the Ministry of Economy and Competitiveness (MINECO) of Spain Project Fine-scale structure of cross-shore GRADIENTS along the Mediterranean coast (CTM2012-39476) and SifoMED (CTM2017-83774-P). P.M. Salgado-Hernanz, was supported by a Ph.D. Doctoral research fellowship FPI (*Formación Personal Investigación*) fellowship BES-2013-067305 from MINECO.

References

- 640 Amante, C. and Eakins, B. W.: ETOPO1 1 Arc-Minute global relief model: Procedures, data sources and analysis, NOAA Tech. Memo. NESDIS NGDC-24, (March), 19, doi:10.1594/PANGAEA.769615, 2009.
- Antoine, D. and André, M.: Algal pigment distribution and primary production in the eastern Mediterranean as derived from coastal zone color scanner observations, *J. Geophys. Reserach*, 100, 193–209, 1995.
- Antoine, D. and Morel, A.: Oceanic primary production, 1. Adaptation of a spectral light-photosynthesis model in view of application to satellite chlorophyll observations, *Global Biogeochem. Cycles*, 10, 43–55, 1996.
- 645 Antoine, D., André, J.-M. and Morel, A.: Antoine, André, Morel - 1996 - Oceanic primary production 2. Estimation at global scale from satellite (Coastal Zone Color Scanner), *Global Biogeochem. Cycles*, 10, 57–69, 1996.
- Barale, V., Jaquet, J. M. and Ndiaye, M.: Algal blooming patterns and anomalies in the Mediterranean Sea as derived from the SeaWiFS data set (1998-2003), *Remote Sens. Environ.*, 112(8), 3300–3313, doi:10.1016/j.rse.2007.10.014, 2008.
- 650 Basterretxea, G., Tovar-Sanchez, A., Beck, A. J., Masqué, P., Bokuniewicz, H. J., Coffey, R., Duarte, C. M., Garcia-Orellana, J., Garcia-Solsona, E., Martinez-Ribes, L. and Vaquer-Sunyer, R.: Submarine groundwater discharge to the coastal environment of a Mediterranean island (Majorca, Spain): Ecosystem and biogeochemical significance, *Ecosystems*, 13(5), 629–643, doi:10.1007/s10021-010-9334-5, 2010.
- Basterretxea, G., Font-Muñoz, J. S., Salgado-Hernanz, P. M., Arrieta, J. and Hernández-Carrasco, I.: Patterns of chlorophyll interannual variability in Mediterranean biogeographical regions, *Remote Sens. Environ.*, 215(May), 7–17, doi:10.1016/j.rse.2018.05.027, 2018.
- 655 Bauer, J. E., Cai, W., Raymond, P. A., Bianchi, T. S., Hopkinson, C. S. and Regnier, P. A. G.: The changing carbon cycle of the coastal ocean, *Nature*, 504, 1–10, doi:10.1038/nature12857, 2013.

- Behrenfeld, M. J., O'Malley, R. T., Siegel, D. A., McClain, C. R., Sarmiento, J. L., Feldman, G. C., Milligan, A. J., Falkowski, P. G., Letelier, R. M. and Boss, E. S.: Climate-driven trends in contemporary ocean productivity, *Nature*, 444(7120), 752–755, doi:10.1038/nature05317, 2006.
- Béjaoui, B., Ben Ismail, S., Othmani, A., Ben Abdallah-Ben Hadj Hamida, O., Chevalier, C., Feki-Sahnoun, W., Harzallah, A., Ben Hadj Hamida, N., Bouaziz, R., Dahech, S., Diaz, F., Tounsi, K., Sammari, C., Pagano, M. and Bel Hassen, M.: Synthesis review of the Gulf of Gabes (eastern Mediterranean Sea, Tunisia): Morphological, climatic, physical oceanographic, biogeochemical and fisheries features, *Estuar. Coast. Shelf Sci.*, 219(January), 395–408, doi:10.1016/j.ecss.2019.01.006, 2019.
- Belgrano, A., Lindahl, O. and Hernroth, B.: North Atlantic Oscillation primary productivity and toxic phytoplankton in the Gullmar Fjord, Sweden (1986-1996), *R. Soc. Publ.*, 266(1418), 425–430, 2008.
- Berthon, J. F. and Zibordi, G.: Bio-optical relationships for the northern Adriatic Sea, *Int. J. Remote Sens.*, 25(7–8), 1527–1532, doi:10.1080/01431160310001592544, 2004.
- Bethoux, J. P.: Oxygen consumption, new production, vertical advection and environmental evolution in the Mediterranean Sea, *Deep Sea Res. Part A, Oceanogr. Res. Pap.*, 36(5), 769–781, doi:10.1016/0198-0149(89)90150-7, 1989.
- Béthoux, J. P., Morin, P., Chaumery, C., Connan, O., Gentili, B. and Ruiz-Pino, D.: Nutrients in the Mediterranean Sea, mass balance and statistical analysis of concentrations with respect to environmental change, *Mar. Chem.*, 63(1–2), 155–169, doi:10.1016/S0304-4203(98)00059-0, 1998.
- Beusen, A. H. W., Bouwman, A. F., Van Beek, L. P. H., Mogollón, J. M. and Middelburg, J. J.: Global riverine N and P transport to ocean increased during the 20th century despite increased retention along the aquatic continuum, *Biogeosciences*, 13(8), 2441–2451, doi:10.5194/bg-13-2441-2016, 2016.
- Boldrin, A., Miserocchi, S., Rabitti, S., Turchetto, M. M., Balboni, V. and Socal, G.: Particulate matter in the southern Adriatic and Ionian Sea: Characterisation and downward fluxes, *J. Mar. Syst.*, 33–34, 389–410, doi:10.1016/S0924-7963(02)00068-4, 2002.
- Bosc, E., Bricaud, A. and Antoine, D.: Seasonal and interannual variability in algal biomass and primary production in the Mediterranean Sea, as derived from 4 years of SeaWiFS observations, *Global Biogeochem. Cycles*, 18(1), 1–17, doi:10.1029/2003gb002034, 2004.
- Bricaud, A., Bosc, E. and Antoine, D.: Algal biomass and sea surface temperature in the Mediterranean Basin, *Remote Sens. Environ.*, 81(2–3), 163–178, doi:10.1016/S0034-4257(01)00335-2, 2002.
- Cai, W.: Estuarine and coastal ocean Carbon paradox: CO₂ sinks or sites of terrestrial carbon incineration?, *Ann. Rev. Mar. Sci.*, 3, 123–45, doi:10.1146/annurev-marine-120709-142723, 2011.
- Campbell, J., Antoine, D., Armstrong, R., Arrigo, K., Balch, W., Barber, R., Behrenfeld, M., Bidigare, R., Bishop, J., Carr, M., Esaias, W., Falkowski, P., Hoepffner, N., Iverson, R., Kiefer, D., Lohrenz, S. and Marra, J.: Comparison of algorithms for estimating ocean primary production from surface chlorophyll , temperature , and irradiance, *Glob. Biochem. Cycles*, 16(3), 2002.
- Capuzzo, E., Lynam, C. P., Barry, J., Stephens, D., Forster, R. M., Greenwood, N., McQuatters-Gollop, A., Silva, T., van

- Leeuwen, S. M. and Engelhard, G. H.: A decline in primary production in the North Sea over 25 years, associated with reductions in zooplankton abundance and fish stock recruitment, *Glob. Chang. Biol.*, 24(1), e352–e364, doi:10.1111/gcb.13916, 2018.
- 695
- Carlson, C. A., Bates, N. R., Hansell, D. A. and Steinberg, D. K.: Carbon cycle, in *Encyclopedia of Ocean Sciences*, vol. 1, pp. 390–400, Elsevier Ltd., 2001.
- Carr, M. E., Friedrichs, M. A. M., Schmeltz, M., Noguchi Aita, M., Antoine, D., Arrigo, K. R., Asanuma, I., Aumont, O., Barber, R., Behrenfeld, M., Bidigare, R., Buitenhuis, E. T., Campbell, J., Ciotti, A., Dierssen, H., Dowell, M., Dunne, J., Esaias, W., Gentili, B., Gregg, W., Groom, S., Hoepffner, N., Ishizaka, J., Kameda, T., Le Quéré, C., Lohrenz, S., Marra, J., Mélin, F., Moore, K., Morel, A., Reddy, T. E., Ryan, J., Scardi, M., Smyth, T., Turpie, K., Tilstone, G., Waters, K. and Yamanaka, Y.: A comparison of global estimates of marine primary production from ocean color, *Deep. Res. Part II Top. Stud. Oceanogr.*, 53(5–7), 741–770, doi:10.1016/j.dsr2.2006.01.028, 2006.
- 700
- Cebrian, J.: Variability and control of carbon consumption, export, and accumulation in marine communities, *Limnol. Oceanogr.*, 47(1), 11–22, 2002.
- 705
- Charantonis, A. A., Badran, F. and Thiria, S.: Retrieving the evolution of vertical profiles of Chlorophyll-a from satellite observations using Hidden Markov Models and Self-Organizing Topological Maps, *Remote Sens. Environ.*, 163, 229–239, doi:10.1016/j.rse.2015.03.019, 2015.
- Chassot, E., Bonhommeau, S., Dulvy, N. K., Mélin, F., Watson, R., Gascuel, D. and Le Pape, O.: Global marine primary production constrains fisheries catches, *Ecol. Lett.*, 13, 495–505, doi:10.1111/j.1461-0248.2010.01443.x, 2010.
- 710
- Chavez, F. P., Messi, M. and Pennington, J. T.: Marine primary production in relation to climate variability and change, *Annu. Rev. of Marine Sci.*, 3, 227–260, doi:10.1146/annurev.marine.010908.163917, 2011.
- Civitaresse, G., Gačić, M., Lipizer, M. and Eusebi Borzelli, G. L.: On the impact of the Bimodal Oscillating System (BiOS) on the biogeochemistry and biology of the Adriatic and Ionian Seas (Eastern Mediterranean), *Biogeosciences*, 7(12), 3987–3997, doi:10.5194/bg-7-3987-2010, 2010.
- 715
- Cloern, J. E. and Jassby, A. D.: Complex seasonal patterns of primary producers at the land-sea interface, *Ecol. Lett.*, 11(12), 1294–1303, doi:10.1111/j.1461-0248.2008.01244.x, 2008.
- Cloern, J. E., Jassby, A. D., Thompson, J. K. and Hieb, K. A.: A cold phase of the East Pacific triggers new phytoplankton blooms in San Francisco Bay, *Proc. Natl. Acad. Sci. U. S. A.*, 104(47), 18561–18565, doi:10.1073/pnas.0706151104, 2007.
- 720
- Cole, J. J., Prairie, Y. T., Caraco, N. F., McDowell, W. H., Tranvik, L. J., Striegl, R. G., Duarte, C. M., Kortelainen, P., Downing, J. A., Middelburg, J. J. and Melack, J.: Plumbing the global carbon cycle: Integrating inland waters into the terrestrial carbon budget, *Ecosystems*, 10, 171–184, doi:10.1007/s10021-006-9013-8, 2007.
- Colella, S., D’Ortenzio, F., Marullo, S., Santoleri, R., Ragni, M. and D’Alcala, M. R.: Primary production variability in the Mediterranean Sea from SeaWiFS data, in *Primary production variability in the Mediterranean Sea from SeaWiFS data*, vol. 5233, pp. 371–383, *Proceedings of SPIE - The International Society for Optical Engineering.*, 2003.
- 725
- Colella, S., Falcini, F., Rinaldi, E., Sammartino, M. and Santoleri, R.: Mediterranean ocean colour chlorophyll trends, *PLoS*

- One, 11(6), 1–16, doi:10.1371/journal.pone.0155756, 2016.
- Coll, M., Piroddi, C., Steenbeek, J. G., Kaschner, K., Frogli, C., Guilhaumon, F., Coll, M., Piroddi, C., Steenbeek, J., Kaschner, K., Ben, F., Lasram, R., Ballesteros, E., Bianchi, C. N., Corbera, J., Dailianis, T., Kesner-reyes, K., Kitsos, M., Rius-barile, J., Martin, D., Mouillot, D., Oro, D., Turon, X., Villanueva, R. and Voultsiadou, E.: The biodiversity of the Mediterranean Sea: Estimates, patterns and threats, *PLoS One*, 5(August 2010), doi:10.1371/journal.pone.0011842, 2010.
- 730 Conan, P., Pujó-Pay, M., Raimbault, P. and Leveau, M.: Variabilité hydrologique et biologique du golfe du Lion . II . Productivité sur le bord interne du courant, *Oceanol. Acta*, 21, 767–782, doi:10.1016/S0399-1784(99)80004-8, 1998.
- Conley, D. J., Paerl, H. W., Howarth, R. W., Boesch, D. F., Seitzinger, S. P., Havens, K. E., Lancelot, C. and Likens, G. E.: Controlling Eutrophication : Nitrogen and Phosphorus, *Science* (80-), 323, 2009.
- 735 Cramer, W., Guiot, J., Fader, M., Garrabou, J., Gattuso, J. P., Iglesias, A., Lange, M. A., Lionello, P., Llasat, M. C., Paz, S., Peñuelas, J., Snoussi, M., Toreti, A., Tsimplis, M. N. and Xoplaki, E.: Climate change and interconnected risks to sustainable development in the Mediterranean, *Nat. Clim. Chang.*, 8(11), 972–980, doi:10.1038/s41558-018-0299-2, 2018.
- Criado-Aldeanueva, F. and Soto-Navarro, F. J.: The mediterranean oscillation teleconnection index: Station-based versus principal component paradigms, *Adv. Meteorol.*, 2013, doi:10.1155/2013/738501, 2013.
- 740 Cushman-Roisin, B., Gačić, M., Poulain, P.-M. P.-M. and Artegiani, A.: Physical Oceanography of the Adriatic Sea. Past, Present and Future, Kluwer Academic Publishers., 2001.
- D’Alimonte, D. and Zibordi, G.: Phytoplankton determination in an optically complex coastal region using a multilayer perceptron neural network, *IEEE Trans. Geosci. Remote Sens.*, 41(12 PART I), 2861–2868, doi:10.1109/TGRS.2003.817682, 2003.
- 745 Deegan, L. A., Johnson, D. S., Warren, R. S., Peterson, B. J., Fleeger, J. W., Fagherazzi, S. and Wollheim, W. M.: Coastal eutrophication as a driver of salt marsh loss, *Nature*, 490(7420), 388–392, doi:10.1038/nature11533, 2012.
- Dekker, A., Brando, V. and Abste, J.: Seagrasses: Biology, ecology and conservation, in *Seagrasses: Biology, Ecology and Conservation*, edited by A. W. D. Larkum, pp. 347–359, Springer., 2007.
- 750 Djakovac, T., Degobbi, D., Supic, N., Precali, R., Supić, N. and Precali, R.: Marked reduction of eutrophication pressure in the northeastern Adriatic in the period 2000–2009, *Estuar. Coast. Shelf Sci.*, 115, 25–32, doi:10.1016/j.ecss.2012.03.029, 2012.
- Drira, Z., Hamza, A., Belhassen, M. and Ayadi, H.: Dynamics of dinoflagellates and environmental factors during the summer in the Gulf of Gabes (Tunisia , Eastern Mediterranean Sea), *Sci. Mar.*, 72(March), 59–71, 2008.
- Ducklow, H. W., Steinberg, D. K. and Buesseler, K. O.: Upper ocean carbon export and the Biological Pump, *Oceanography*, 14(4), 50–58, 2001.
- 755 Dunne, J. P., Sarmiento, J. L. and Gnanadesikan, A.: A synthesis of global particle export from the surface ocean and cycling through the ocean interior and on the seafloor, *Glob. Biochem. Cycles*, 21(July), 1–16, doi:10.1029/2006GB002907, 2007.
- Durrieu De Madron, X., Houpert, L., Puig, P., Sanchez-Vidal, A., Testor, P., Bosse, A., Estournel, C., Somot, S., Bourrin, F., Bouin, M. N., Beauverger, M., Beguery, L., Calafat, A., Canals, M., Cassou, C., Coppola, L., Dausse, D., D’Ortenzio, F., Font, J., Heussner, S., Kunesch, S., Lefevre, D., Le Goff, H., Martín, J., Mortier, L., Palanques, A. and Raimbault, P.: Interaction of
- 760

- dense shelf water cascading and open-sea convection in the northwestern Mediterranean during winter 2012, *Geophys. Res. Lett.*, 40(7), 1379–1385, doi:10.1002/grl.50331, 2013.
- EEA: Europe's Environment - The Dobris Assessment, [online] Available from: <https://www.eea.europa.eu/publications/92-826-5409-5>, 1995.
- 765 Efthymiadis, D., Goodess, C. M. and Jones, P. D.: Trends in Mediterranean gridded temperature extremes and large-scale circulation influences, *Nat. Hazards Earth Syst. Sci.*, 11(8), 2199–2214, doi:10.5194/nhess-11-2199-2011, 2011.
- Estrada, M.: Primary production in the northwestern Mediterranean, *Sci. Mar.*, 60(SUPPL. 2), 55–64, 1996.
- Farikou, O., Sawadogo, S., Niang, A., Diouf, D., Brajard, J., Mejia, C., Dandonneau, Y., Gasc, G., Crepon, M. and Thiria, S.: Inferring the seasonal evolution of phytoplankton groups in the Senegalo-Mauritanian upwelling region from satellite ocean-
- 770 color spectral measurements, *J. Geophys. Res. Ocean.*, 120(9), 6581–6601, doi:10.1002/2015JC010738, 2015.
- Field, C. B., Behrenfeld, M. J. and Randerson, J. T.: Primary Production of the biosphere: Integrating terrestrial and oceanic components, *Science* (80-.), 281, 237–240, doi:10.1126/science.281.5374.237, 1998.
- Friedrichs, M. A. M., Carr, M., Barber, R. T., Scardi, M., Antoine, D., Armstrong, R. A., Asanuma, I., Behrenfeld, M. J., Buitenhuis, E. T., Chai, F., Christian, J. R., Ciotti, A. M., Doney, S. C., Dowell, M., Dunne, J., Gentili, B., Gregg, W.,
- 775 Hoepffner, N., Ishizaka, J., Kameda, T., Lima, I., Marra, J., Mélin, F., Moore, J. K., Morel, A., Malley, R. T. O., Reilly, J. O., Saba, V. S., Schmeltz, M., Smyth, T. J., Tjiputra, J., Waters, K., Westberry, T. K. and Winguth, A.: Assessing the uncertainties of model estimates of primary productivity in the tropical Pacific Ocean, *J. Mar. Syst.*, 76(1–2), 113–133, doi:10.1016/j.jmarsys.2008.05.010, 2009.
- Garcia-gorritz, E. and Carr, M. E.: Physical control of phytoplankton distributions in the Alboran Sea: A numerical and satellite
- 780 approach, *J. Geophys. Res. Ocean.*, 106(C8), 16795–16805, doi:10.1029/1999jc000029, 2001.
- Gasol, J. M., Cardelús, C., Morán, X. A. G., Balagué, V., Forn, I., Marrasé, C., Massana, R., Pedrós-Alió, C., Sala, M. M., Simó, R., Vaqué, D. and Estrada, M.: Seasonal patterns in phytoplankton photosynthetic parameters and primary production at a coastal NW Mediterranean site | Regularidades estacionales en la producción primaria y los parámetros fotosintéticos en una estación costera del NO Mediterráneo, *Sci. Mar.*, 80(September), 63–77, doi:10.3989/scimar.04480.06E, 2016.
- 785 Gattuso, J. P., Frankignoulle, M. and Wollast, R.: Carbon and carbonate metabolism in coastal aquatic ecosystems, *Annu. Rev. Ecol. Syst.*, 29, 405–434, doi:10.1146/annurev.ecolsys.29.1.405, 1998.
- Giani, M., Djakovac, T., Degobbi, D., Cozzi, S., Solidoro, C. and Umani, S. F.: Recent changes in the marine ecosystems of the northern Adriatic Sea, *Estuar. Coast. Shelf Sci.*, 115, 1–13, doi:10.1016/j.ecss.2012.08.023, 2012.
- Goffart, A., Hecq, J. H. and Legendre, L.: Changes in the development of the winter-spring phytoplankton bloom in the Bay
- 790 of Calvi (NW Mediterranean) over the last two decades: A response to changing climate?, *Mar. Ecol. Prog. Ser.*, 236(August 2015), 45–60, doi:10.3354/meps236045, 2002.
- Grbec, B., Morović, M., Beg Paklar, G., Kušpilić, G., Matijević, S., Matić, F. and Gladan, Ž. N.: The relationship between the atmospheric variability and productivity in the adriatic Sea area, *J. Mar. Biol. Assoc. United Kingdom*, 89(8), 1549–1558, doi:10.1017/S0025315409000708, 2009.

- 795 Gregg, W. W., Conkright, M. E., Ginoux, P., O'Reilly, J. E. and Casey, N. W.: Ocean primary production and climate: Global decadal changes, *Geophys. Res. Lett.*, 30(15), 10–13, doi:10.1029/2003GL016889, 2003.
- Hamza-Chaffai, A., Amiard-Triquet, C. and El Abed, A.: Metallothionein-like protein: Is it an efficient biomarker of metal contamination? A case study based on fish from the Tunisian coast, *Arch. Environ. Contam. Toxicol.*, 33(1), 53–62, doi:10.1007/s002449900223, 1997.
- 800 Henson, S. A., Sarmiento, J. L., Dunne, J. P., Bopp, L., Lima, I., Doney, S. C., John, J. and Beaulieu, C.: Detection of anthropogenic climate change in satellite records of ocean chlorophyll and productivity, *Biogeosciences*, 7(2), 621–640, doi:10.5194/bg-7-621-2010, 2010.
- Herut, B., Collier, R. and Krom, M. D.: The role of dust in supplying nitrogen and phosphorus to the Southeast Mediterranean, *Limnol. Oceanogr.*, 47(3), 870–878, doi:10.4319/lom.2002.47.3.0870, 2002.
- 805 Hurrell, J. W.: Decadal trends in the North Atlantic Oscillation: Regional temperatures and precipitation, *Science* (80-.), 269, 7–10, 1995.
- Hurrell, J. W. and Van Loon, H.: Decadal variations in climate associated with the North Atlantic oscillation, *Clim. Change*, 36(3–4), 301–326, doi:10.1023/a:1005314315270, 1997.
- Kahru, M., Brotas, V., Manzano-Sarabia, M. and Mitchell, B. G.: Are phytoplankton blooms occurring earlier in the Arctic?, *Glob. Chang. Biol.*, 17(4), 1733–1739, doi:10.1111/j.1365-2486.2010.02312.x, 2011.
- 810 Katlane, R., Nechad, B., Ruddick, K. and Zargouni, F.: Optical remote sensing of turbidity and total suspended matter in the Gulf of Gabes, *Arab. J. Geosci.*, 6(5), 1527–1535, doi:10.1007/s12517-011-0438-9, 2011.
- Kohonen, T.: Self-organized Formation of topologically correct feature maps, *Biol. Cybern.*, 43(1), 59–69, doi:10.1007/BF00337288, 1982.
- 815 Kohonen, T.: *Self-Organizing Maps*, Springer-Verlag, Berlin Heidelberg. [online] Available from: <https://www.springer.com/gp/book/9783540679219>, 2001.
- Komatsu, T.: *A manual for seagrass and seaweed beds distribution mapping with satellite images.*, 2015.
- Kress, N. and Herut, B.: Spatial and seasonal evolution of dissolved oxygen and nutrients in the Southern Levantine Basin (Eastern Mediterranean Sea): Chemical characterization of the water masses and inferences on the N : P ratios, *Deep. Res. Part*
- 820 *I Oceanogr. Res. Pap.*, 48(11), 2347–2372, doi:10.1016/S0967-0637(01)00022-X, 2001.
- Lacroix, G. and Nival, P.: Influence of meteorological variability on primary production dynamics in the Ligurian Sea (NW Mediterranean Sea) with a 1D hydrodynamic/biological model, *J. Mar. Syst.*, 16(1–2), 23–50, doi:10.1016/S0924-7963(97)00098-5, 1998.
- Laws, E. A., Falkowski, P. G., Smith, W. O., Ducklow, H. and McCarthy, J. J.: Temperature effects on export production in
- 825 the open ocean, *Global Biogeochem. Cycles*, 14(4), 1231–1246, doi:10.1029/1999GB001229, 2000.
- Laws, E. A., D'Sa, E. and Naik, P.: Simple equations to estimate ratios of new or export production to total production from satellite-derived estimates of sea surface temperature and primary production, *Limnol. Oceanogr. Methods*, 9(DECEMBER), 593–601, doi:10.4319/lom.2011.9.593, 2011.

- Lazzari, P., Solidoro, C., Ibello, V., Salon, S., Teruzzi, A., Béranger, K., Colella, S. and Crise, A.: Seasonal and inter-annual variability of plankton chlorophyll and primary production in the Mediterranean Sea: A modelling approach, *Biogeosciences*, 9(1), 217–233, doi:10.5194/bg-9-217-2012, 2012.
- Lionello, P. and Scarascia, L.: The relation between climate change in the Mediterranean region and global warming, *Reg. Environ. Chang.*, 18(5), 1481–1493, doi:10.1007/s10113-018-1290-1, 2018.
- Liu, K.-K., Iseki, K. and Chao, Y.: Continental margin carbon fluxes, in *The Changing Ocean Carbon Cycle: A Midterm Synthesis of the Joint Global Ocean Flux Study*, edited by R. B. Hanson, H. W. Ducklow, and J. G. Field, Cambridge University Press., 2000.
- Liu, Y. and Weisberg, R. H.: Patterns of ocean current variability on the West Florida Shelf using the self-organizing map, *J. Geophys. Res. Ocean.*, 110(6), 1–12, doi:10.1029/2004JC002786, 2005.
- Liu, Y., Weisberg, R. H. H. and Mooers, C. N. K. N. K.: Performance evaluation of the self-organizing map for feature extraction, *J. Geophys. Res. Ocean.*, 111(5), 1–14, doi:10.1029/2005JC003117, 2006.
- Lohrenz, S. E., Wiesenburg, D. A., DePalma, I. P., Johnson, K. S. and Gustafson, D. E.: Interrelationships among primary production, chlorophyll, and environmental conditions in frontal regions of the western Mediterranean Sea, *Deep Sea Res. Part A, Oceanogr. Res. Pap.*, 35(5), 793–810, doi:10.1016/0198-0149(88)90031-3, 1988.
- Lopez-bustins, J. A., Sánchez- Lorenzo, A., Azorin-molina, C. and Ordóñez-López, A.: Tendencias de la precipitación invernal en la fachada oriental de la Península Ibérica, *EGU/AGU Sess. Earth Radiat. budget, Radiat. forcing Clim. Chang.*, 2008.
- Ludwig, W., Dumont, E., Meybeck, M. and Heussner, S.: River discharges of water and nutrients to the Mediterranean and Black Sea: Major drivers for ecosystem changes during past and future decades?, *Prog. Oceanogr.*, 80(3–4), 199–217, doi:10.1016/j.pocean.2009.02.001, 2009.
- Macias, D., Garcia-Gorrioz, E. and Stips, A.: Major fertilization sources and mechanisms for Mediterranean Sea coastal ecosystems, *Limnol. Oceanogr.*, 63(2), 897–914, doi:10.1002/lno.10677, 2017.
- Macias, D. M., Garcia-Gorrioz, E. and Stips, A.: Productivity changes in the Mediterranean Sea for the twenty-first century in response to changes in the regional atmospheric forcing, *Front. Mar. Sci.*, 2(OCT), 1–13, doi:10.3389/fmars.2015.00079, 2015.
- Marshall, J., Kushnir, Y., Battisti, D., Chang, P., Czaja, A., Dickson, R., Hurrell, J., McCartney, M., Saravanan, R., Visbeck, M., Robert, D., Hurrell, J., McCartney, M., Saravanan, R. and Visbeck, M.: Review: North Atlantic climate variability: Phenomena, impacts and mechanisms, *Int. J. Climatol.*, 21(15), 1863–1898, doi:10.1002/joc.693, 2001.
- Martínez-Asensio, A., Marcos, M., Tsimplis, M. N., Gomis, D., Josey, S. and Jordà, G.: Impact of the atmospheric climate modes on Mediterranean sea level variability, *Glob. Planet. Change*, 118, 1–15, doi:10.1016/j.gloplacha.2014.03.007, 2014.
- Marty, J. C.: The DYFAMED time-series program (French-JGOFS), *Deep. Res. Part II Top. Stud. Oceanogr.*, 49(11), 1963–1964, doi:10.1016/S0967-0645(02)00021-8, 2002.
- Marty, J. C., Chiavérini, J., Pizay, M. D. and Avril, B.: Seasonal and interannual dynamics of nutrients and phytoplankton pigments in the western Mediterranean Sea at the DYFAMED time-series station (1991-1999), *Deep. Res. Part II Top. Stud. Oceanogr.*, 49(11), 1965–1985, doi:10.1016/S0967-0645(02)00022-X, 2002.

- Marty, J. C. C. and Chiavérini, J.: Hydrological changes in the Ligurian Sea (NW Mediterranean, DYFAMED site) during 1995-2007 and biogeochemical consequences, *Biogeosciences*, 7(7), 2117–2128, doi:10.5194/bg-7-2117-2010, 2010.
- 865 Massey, F. J., Frank, J. and Maseey, J.: The Kolmogorov-Smirnov Test for Goodness of Fit, *J. Am. Stat. Assoc.*, 46(253), 68–78, doi:10.1016/0378-3758(90)90051-U, 1951.
- Micheli, F., Halpern, B. S., Walbridge, S., Ciriaco, S., Ferretti, F., Fraschetti, S., Lewison, R., Nykjaer, L. and Rosenberg, A. A.: Cumulative human impacts on Mediterranean and Black Sea marine ecosystems: Assessing current pressures and opportunities, *PLoS One*, 8(12), doi:10.1371/journal.pone.0079889, 2013.
- 870 Mihanović, H., Vilibić, I., Carniel, S., Tudor, M., Russo, A., Bergamasco, A., Bubić, N., Ljubešić, Z., Viličić, D., Boldrin, A., Malačić, V., Celio, M., Comici, C. and Raicich, F.: Exceptional dense water formation on the adriatic shelf in the winter of 2012, *Ocean Sci.*, 9(3), 561–572, doi:10.5194/os-9-561-2013, 2013.
- Molinero, J. C., Ibanez, F., Nival, P., Buecher, E. and Souissi, S.: North Atlantic climate and northwestern Mediterranean plankton variability, *Limnol. Oceanogr.*, 50(4), 1213–1220, doi:10.4319/lo.2005.50.4.1213, 2005.
- 875 Morán, X. A. G. A. G. and Estrada, M.: Short-term variability of photosynthetic parameters and particulate and dissolved primary production in the Alboran sea (SW Mediterranean), *Mar. Ecol. Prog. Ser.*, 212, 53–67, doi:10.3354/meps212053, 2001.
- Morel, A.: Light and marine photosynthesis: a spectral model with geochemical and climatological implications, *Prog. Oceanogr.*, 26(3), 263–306, doi:10.1016/0079-6611(91)90004-6, 1991.
- 880 Morel, A. and André, J.-M.: Pigment distribution and primary production in the Western Mediterranean as derived and modeled from Coastal Zone Color Scanner Observations, *J. Geophys. Res.*, 96(C7), 685–698, doi:10.1029/95JC00466, 1991.
- Morel, A. and Berthon, J.-F.: Surface pigments, algal biomass profiles, and potential production of the euphotic layer: Relationships reinvestigated in view of remote-sensing applications, *Limnol. Oceanogr.*, 34(8), 1545–1562, doi:10.4319/lo.1989.34.8.1545, 1989.
- 885 Morel, A. and Maritorena, S.: Bio-optical properties of oceanic waters: A reappraisal, *J. Geophys. Res. Ocean.*, 106(C4), 7163–7180, doi:10.1029/2000jc000319, 2001.
- Morel, A., Antoine, D., Babin, M. and Dandonneau, Y.: Measured and modeled primary production in the northeast Atlantic (EUMELI JGOFS program): The impact of natural variations in photosynthetic parameters on model predictive skill, *Deep. Res. Part I Oceanogr. Res. Pap.*, 43(8), 1273–1304, doi:10.1016/0967-0637(96)00059-3, 1996.
- 890 Morel, A., Gentili, B., Chami, M. and Ras, J.: Bio-optical properties of high chlorophyll Case 1 waters and of yellow-substance-dominated Case 2 waters, *Deep. Res. Part I Oceanogr. Res. Pap.*, 53(9), 1439–1459, doi:10.1016/j.dsr.2006.07.007, 2006.
- Moutin, T. and Raimbault, P.: Primary production, carbon export and nutrients availability in western and eastern Mediterranean Sea in early summer 1996 (MINOS cruise), *J. Mar. Syst.*, 33–34, 273–288, doi:10.1016/S0924-7963(02)00062-3, 2002.
- 895 Muller-Karger, F. E., Varela, R., Thunell, R., Luerssen, R., Hu, C. and Walsh, J. J.: The importance of continental margins in the global carbon cycle, *Geophys. Res. Lett.*, 32(December 2004), 10–13, doi:10.1029/2004GL021346, 2005.

- Ben Mustapha, Z., Alvain, S., Jamet, C., Loisel, H. and Dessailly, D.: Automatic classification of water-leaving radiance anomalies from global SeaWiFS imagery: Application to the detection of phytoplankton groups in open ocean waters, *Remote Sens. Environ.*, 146, 97–112, doi:10.1016/j.rse.2013.08.046, 2014.
- 900 Nixon, S. W.: Replacing the Nile: Are anthropogenic nutrients providing the fertility once brought to the Mediterranean by a great river?, *Ambio A J. Hum. Environ.*, 32(1), 30–39, doi:10.1579/0044-7447-32.1.30, 2003.
- Nixon, S. W.: The Artificial Nile: The Aswan High Dam blocked and diverted nutrients and destroyed a Mediterranean fishery, but human activities may have revived it, *Am. Sci.*, 92(2), 158–165, 2004.
- Nykjaer, L.: Mediterranean Sea surface warming 1985 – 2006, *Clim. Resea*, 39(December 1990), 11–17, doi:10.3354/cr00794,
905 2009.
- O'Reilly, J. and Sherman, K.: Chapter 5.1. Primary productivity patterns and trends, United Nations Environment Programme, Nairobi., 2016.
- Pace, M. L., Knauer, G. A., Karl, D. M. and Martin, J. H.: Primary production, new production and vertical flux in the eastern Pacific Ocean, *Nature*, 325, 1987.
- 910 Paerl, H. w., Willey, J. D., Go, M., Peierls, B. L., Pinckney, J. L. and Fogel, M. L.: Rainfall stimulation of primary production in western Atlantic Ocean waters : roles of different nitrogen sources and CO-limiting nutrients, *Mar. Ecol. Prog. Ser.*, 176, 205–214, 1999.
- Palutikof, J.: Analysis of Mediterranean Climate Data: Measured and Modelled, in *Mediterranean Climate: Variability and Trends*, edited by H. J. Bolle, pp. 125–132, Springer-Verlag Berlin Heidelberg., 2003.
- 915 Pastor, F., Valiente, J. A. A., Palau, J. L. and Luis Palau, J.: Sea Surface Temperature in the Mediterranean: Trends and Spatial Patterns (1982–2016), *Pure Appl. Geophys.*, 175(11), 4017–4029, doi:10.1007/s00024-017-1739-z, 2018.
- Pauly, D. and Christensen, V.: Primary production required to sustain global fisheries, *Lett. to Nat.*, 374(March), 255–257, 1995.
- Pauly, D., Christensen, V., Guénette, S., Pitcher, T. J., Sumaila, U. R., Walters, C. J., Watson, R. and Zeller, D.: Towards
920 sustainability in world fisheries, *Nat. Publ. Gr.*, 418(August), 689–695, 2002.
- Pinardi, N., Zavatarelli, M., Arneri, E., Crise, A. and Ravaioli, M.: Chapter 32. The physical, sedimentary and ecological structure and variability of shelf areas in the Mediterranean Sea (27,S), in *The Sea. The Global Coastal Ocean*, vol. 14, edited by A. R. Robinson and K. H. Brink, pp. 1243–1272., 2006.
- Piroddi, C., Coll, M., Liqueste, C., Macias, D., Greer, K., Buszowski, J., Steenbeek, J., Danovaro, R. and Christensen, V.:
925 Historical changes of the Mediterranean Sea ecosystem: Modelling the role and impact of primary productivity and fisheries changes over time, *Sci. Rep.*, 7(September 2016), 1–18, doi:10.1038/srep44491, 2017.
- Powley, H. R., Dürr, H. H., Lima, A. T., Krom, M. D. and Van Cappellen, P.: Direct Discharges of Domestic Wastewater are a Major Source of Phosphorus and Nitrogen to the Mediterranean Sea, *Environ. Sci. Technol.*, 50(16), 8722–8730, doi:10.1021/acs.est.6b01742, 2016.
- 930 Puggnetti, A., Bazzoni, A. M., Beran, A., Bernardi Aubry, F., Camatti, E., Celussi, M., Coppola, J., Crevatin, E., Del Negro, P.

- and Paoli, A.: Changes in biomass structure and trophic status of the plankton communities in a highly dynamic ecosystem (Gulf of Venice, Northern Adriatic Sea), *Mar. Ecol.*, 29(3), 367–374, doi:10.1111/j.1439-0485.2008.00237.x, 2008.
- Rahav, E., Herut, B., Levi, A., Mulholland, M. R. and Berman-Frank, I.: Springtime contribution of dinitrogen fixation to primary production across the Mediterranean Sea, *Ocean Sci.*, 9(3), 489–498, doi:10.5194/os-9-489-2013, 2013.
- 935 Raicich, F., Malacic, V., Celio, M., Giaiotti, D., Cantoni, C., Colucci, R. R., Cermelj, B. and Pucillo, A.: Extreme air-sea interactions in the Gulf of Trieste (North Adriatic) during the strong Bora event in winter 2012, *J. Geophys. Res. Ocean.*, 118, 5238–5250, doi:10.1002/jgrc.20398, 2013a.
- Raicich, F., Malačič, V., Celio, M., Giaiotti, D., Cantoni, C., Colucci, R. R., Čermelj, B. and Pucillo, A.: Extreme air-sea interactions in the Gulf of Trieste (North Adriatic) during the strong Bora event in winter 2012, *J. Geophys. Res. Ocean.*, 940 118(10), 5238–5250, doi:10.1002/jgrc.20398, 2013b.
- Regaudie-De-Gioux, A., Vaquer-Sunyer, R. and Duarte, C. M.: Patterns in planktonic metabolism in the Mediterranean Sea, *Biogeosciences*, 6(12), 3081–3089, doi:10.5194/bg-6-3081-2009, 2009.
- Rodellas, V., Garcia-Orellana, J., Masqué, P., Feldman, M., Weinstein, Y. and Boyle, E. A.: Submarine groundwater discharge as a major source of nutrients to the Mediterranean Sea, *Proc. Natl. Acad. Sci. U. S. A.*, 112(13), 3926–3930, 945 doi:10.1073/pnas.1419049112, 2015.
- Ryan, J.: Crop nutrients for sustainable agricultural production in the drought-stressed mediterranean region, *J. Agric. Sci. Technol.*, 10(4), 295–306, 2008.
- Saba, V. S. S., Friedrichs, M. A. M. A. M., Antoine, D., Armstrong, R. A. A., Asanuma, I., Behrenfeld, M. J. J., Ciotti, A. M. M., Dowell, M., Hoepffner, N., Hyde, K. J. W., Ishizaka, J., Kameda, T., Marra, J., Mlin, F., Morel, A., O'Reilly, J., Scardi, 950 M., Smith, W. O., Smyth, T. J., Tang, S., Uitz, J., Waters, K. and Westberry, T. K.: An evaluation of ocean color model estimates of marine primary productivity in coastal and pelagic regions across the globe, *Biogeosciences*, 8(2), 489–503, doi:10.5194/bg-8-489-2011, 2011.
- Salgado-Hernanz, P. M., Racault, M. F., Font-Muñoz, J. S. and Basterretxea, G.: Trends in phytoplankton phenology in the Mediterranean Sea based on ocean-colour remote sensing, *Remote Sens. Environ.*, 221(October 2018), 50–64, 955 doi:10.1016/j.rse.2018.10.036, 2019.
- Salmi, T., Maatta, A., Anttila, P., Ruoho-Airola, T. and Amnell, T.: Detecting Trends of Annual Values of Atmospheric Pollutants by the Mann-Kendall Test and Sen's Solpe Estimates the Excel Template Application MAKESENS., 2002.
- Sen, P. K.: Estimates of the regression coefficient based on Kendall ' s Tau Pranab Kumar Sen, *J. Am. Stat. Assoc.*, 63(324), 1379–1389, 1968.
- 960 Simpson, J. H.: Physical processes in the ROFI regime, *J. Mar. Syst.*, 12(1–4), 3–15, doi:10.1016/S0924-7963(96)00085-1, 1997.
- Skoulikidis, N. T., Economou, A. N., Gritzalis, K. C. and Zogaris, S.: Rivers of the Balkans, in *Rivers of Europe*, pp. 421–466, Elsevier Ltd., 2009.
- Smith, S. V. and Hollibaugh, J. T.: Coastal Metabolism and the Oceanic Organic Carbon Balance, *Rev. Geophys.*, 31(92), 75–

965 89, 1993.

Sournia, A.: La production primaire planctonique en Méditerranée: Essai de mise à jour. Bulletin Etude en Commun de la Méditerranée, 5, 128pp., 1973.

Stambler, N.: The Mediterranean Sea – Primary Productivity, in *The Mediterranean Sea: Its history and present challenges*, edited by S. Goffredo and Z. Dubinsky, pp. 113–121, Springer., 2014.

970 Su, L. and Huang, Y.: Seagrass resource assessment using World View-2 imagery in the Redfish Bay, Texas, *J. Mar. Sci. Eng.*, 7(4), doi:10.3390/jmse7040098, 2019.

Tiselius, P., Belgrano, A., Andersson, L. and Lindahl, O.: Primary productivity in a coastal ecosystem: A trophic perspective on a long-term time series, *J. Plankton Res.*, 38(4), 1092–1102, doi:10.1093/plankt/fbv094, 2016.

Törnros, T.: On the relationship between the Mediterranean Oscillation and winter precipitation in the Southern Levant, *Atmos. Sci. Lett.*, 14(4), 287–293, doi:10.1002/asl2.450, 2013.

Tovar-Sánchez, A., Basterretxea, G., Rodellas, V., Sánchez-Quiles, D., García-Orellana, J., Masqué, P., Jordi, A., López, J. M. and Garcia-Solsona, E.: Contribution of groundwater discharge to the coastal dissolved nutrients and trace metal concentrations in Majorca Island: Karstic vs detrital systems, *Environ. Sci. Technol.*, 48(20), 11819–11827, doi:10.1021/es502958t, 2014.

980 Tovar-Sánchez, A., Basterretxea, G., Ben Omar, M., Jordi, A., Sánchez-Quiles, D., Makhani, M., Mouna, D., Muya, C. and Anglès, S.: Nutrients, trace metals and B-vitamin composition of the Moulouya River: A major North African river discharging into the Mediterranean Sea, *Estuar. Coast. Shelf Sci.*, 176, 47–57, doi:10.1016/j.ecss.2016.04.006, 2016.

Trigo, R., Xoplaki, E., Zorita, E., Luterbacher, J., Krichak, S. O., Alpert, P., Jucundus, J., Sáens, J., Fernández, J., González-Rouco, F., Garcia-Herrera, R., Rodo, X., Brunetti, M., Nanni, T., Maugeri, M., Türke, M., Gimeno, L., Ribera, P., Brunet, M., Trigo, I. F., Crepon, M. and Mariotti, A.: Relations between Variability in the Mediterranean Region and Mid-Latitude Variability, in *Developments in Earth and Environmental Sciences: Mediterranean.*, edited by P. Lionello, P. Malanotte-Rizzoli, and R. Boscolo, pp. 179–226, Elsevier., 2006.

985 Turley, C. M.: The changing Mediterranean Sea - A sensitive ecosystem?, *Prog. Oceanogr.*, 44(1–3), 387–400, doi:10.1016/S0079-6611(99)00033-6, 1999a.

990 Turley, C. M.: The changing Mediterranean Sea — a sensitive ecosystem ?, *Prog. Oceanogr.*, 44, 387–400, 1999b.

Uitz, J., Claustre, H., Morel, A. and Hooker, S. B.: Vertical distribution of phytoplankton communities in open ocean: An assessment based on surface chlorophyll, *J. Geophys. Res. Ocean.*, 111(8), doi:10.1029/2005JC003207, 2006.

Uitz, J., Claustre, H., Gentili, B. and Stramski, D.: Phytoplankton class-specific primary production in the world's oceans: Seasonal and interannual variability from satellite observations, *Global Biogeochem. Cycles*, 24(3), 1–19, doi:10.1029/2009GB003680, 2010.

995 Umami, S. F.: Pelagic production and biomass in the Adriatic Sea, *Sci. Mar.*, 60(SUPPL. 2), 65–77, 1996.

Umami, S. F., Del Negro, P., Larato, C., De Vittor, C., Cabrini, M., Celio, M., Falconi, C., Tamberlich, F. and Azam, F.: Major inter-annual variations in microbial dynamics in the Gulf of Trieste (northern Adriatic Sea) and their ecosystem implications,

- Aquat. Microb. Ecol., 46(2), 163–175, doi:10.3354/ame046163, 2007.
- 1000 Vesanto, J., Alhoniemi, E. and Member, S.: Clustering of the Self-Organizing Map, IEEE Trans. neural networks, 11(3), 586–600, 2000a.
- Vesanto, J., Himberg, J., Alhoniemi, E. and Parhankangas, J.: SOM Toolbox for Matlab 5, (Report A57). Hensinki University of Technological, Espoo, Finland., 2000b.
- Vidussi, F., Claustre, H., Manca, B. B., Luchetta, A. and Marty, J.-C.: Phytoplankton pigment distribution in relation to upper
1005 thermocline circulation in the eastern Mediterranean Sea during winter, J. Geophys. Res., 106, 939–956, 2001.
- Volpe, G., Colella, S., Brando, V. E., Forneris, V., La Padula, F., Di Cicco, A., Sammartino, M., Bracaglia, M., Artuso, F. and Santoleri, R.: Mediterranean ocean colour Level 3 operational multi-sensor processing, Ocean Sci., 15(1), 127–146, doi:10.5194/os-15-127-2019, 2019.
- Van Wambeke, F., Lefèvre, D., Prieur, L., Sempéré, R., Bianchi, M., Oubelkheir, K. and Bruyant, F.: Distribution of microbial
1010 biomass, production, respiration, dissolved organic carbon and factors controlling bacterial production across a geostrophic front (Almeria-Oran, SW Mediterranean Sea), Mar. Ecol. Prog. Ser., 269(March 2004), 1–15, doi:10.3354/meps269001, 2004.
- Wang, X. T., Cohen, A. L., Luu, V., Ren, H., Su, Z., Haug, G. H. and Sigman, D. M.: Natural forcing of the North Atlantic nitrogen cycle in the Anthropocene, Proc. Natl. Acad. Sci., 201801049, doi:10.1073/pnas.1801049115, 2018.
- Woodson, C. B. and Litvin, S. Y.: Ocean fronts drive marine fishery production and biogeochemical cycling, Proc. Nat. Acad. Sci. Unites States Am., 112, 1710–1715, doi:10.1073/pnas.1417143112, 2014.
1015
- Zairi, M. and Rouis, M. J.: Impacts environnementaux du stockage du phosphogypse à Sfax (Tunisie), Bull. des Lab. des ponts chaussées, 219, 29–40, 1999.
- Zalidis, G., Stamatiadis, S., Takavakoglou, V., Eskridge, K. and Misopolinos, N.: Impacts of agricultural practices on soil and water quality in the Mediterranean region and proposed assessment methodology, Agric. Ecosyst. Environ., 88(2), 137–146, doi:10.1016/S0167-8809(01)00249-3, 2002.
1020
- Zoppini, A., Pettine, M., Totti, C., Puddu, A., Artegiani, A. and Pagnotta, R.: Nutrients, standing crop and primary production in western coastal waters of the adriatic sea, Estuar. Coast. Shelf Sci., 41(5), 493–513, doi:10.1016/0272-7714(95)90024-1, 1995.

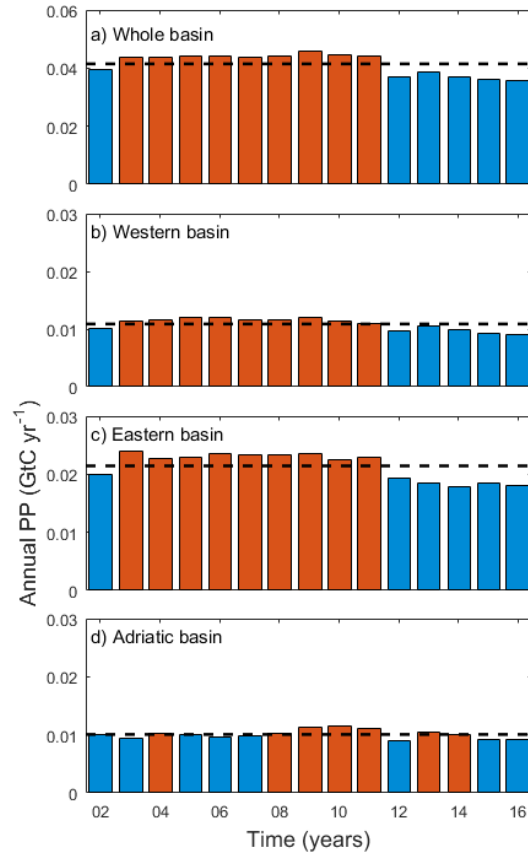
Supplementary Tables

Supp. Table 1: Correlations between the yearly total carbon fixation anomalies for the coastal Mediterranean waters and its sub basins (Σ PP) and its corresponding sea surface temperature (SST).

		NAO index					MOI index				
		Annual	Spring	Summer	Fall	Winter	Annual	Spring	Summer	Fall	Winter
Coastal waters	r	-0,45	0,02	0,02	0,00	0,00	-0,22	0,28	0,02	0,02	0,02
	Pvalue	\leq 0,001	0,60	0,58	0,96	0,97	0,00	0,04	0,62	0,63	0,60
Western coast	r	-0,40	0,00	0,25	0,12	0,02	-0,22	0,08	0,00	0,00	0,00
	Pvalue	\leq 0,001	0,88	0,06	0,20	0,59	0,01	0,31	0,80	0,85	0,96
Eastern coast	r	-0,42	0,02	0,22	0,02	0,00	-0,11	0,02	0,02	0,01	0,04
	Pvalue	\leq 0,001	0,63	0,08	0,59	0,89	0,15	0,62	0,65	0,71	0,46
Adriatic coast	r	-0,31	0,03	0,08	0,00	0,00	-0,38	0,37	0,01	0,00	0,01
	Pvalue	\leq 0,001	0,56	0,30	0,89	0,89	\leq 0,001	0,02	0,74	0,93	0,70

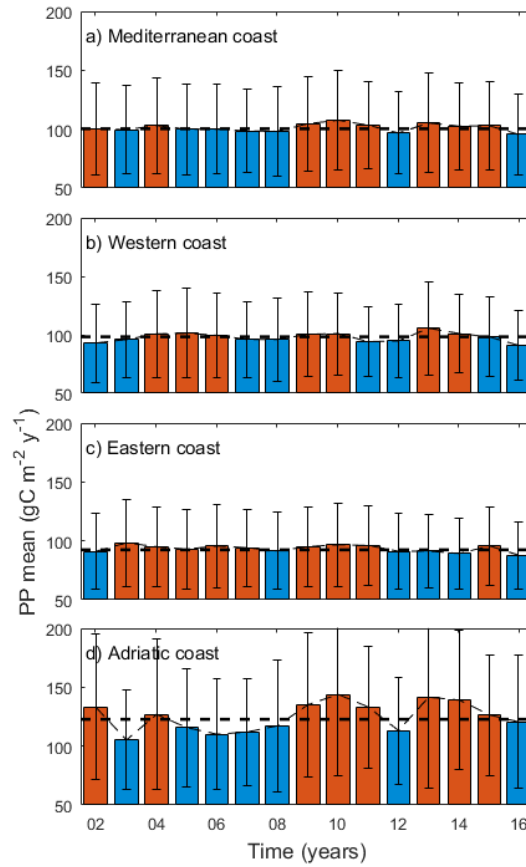
1030

Supplementary figures



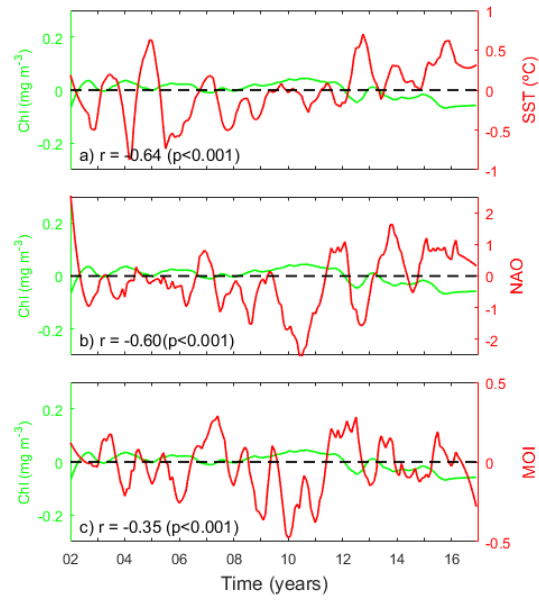
Supp Figure 1. Annual coastal variations in ΣPP (GtC yr⁻¹) for a) the whole Mediterranean Sea, b) the western basin, c) the eastern basin and d) the Adriatic basin. Dash black lines indicate the mean $\Sigma PP_{Coastal}$ for the period 2002-2016 at each study region. Red and blue bars indicate years above and below average values.

1035



1040

Supp Figure 2. Annual variations in $\text{PP}_{\text{annual}}$ (gC m^{-2} per year) for a) the whole Mediterranean Sea, b) the western basin, c) eastern basin and d) the Adriatic coast. Dashed black lines indicate the mean $\text{PP}_{\text{Coastal}}$ at each study region. Red and blue bars indicate years above and below average values.



Supp Figure 3. Relationship between coastal pelagic chlorophyll (Chl anomalies, green lines) and a) SST anomalies, b) NAO index and c) MOI index (red lines).